Los Alamos
NATIONAL LABORATORY
EST 1943

memorandum

Nuclear Engineering and Nonproliferation Division

To/MS: David Hayes, NEN-2, B228
Thru/MS: William Myers, NEN-2, B228 W.L.M.
From/MS: Jesson Hutchinson, NEN-2, B228 JH
Rene Sanchez, NEN-2, B228 RS
Phone/Email: 7-5411/jesson@lanl.gov

Symbol: NEN-2:14-39
Date: October 14, 2014

SUBJECT: TRIP REPORT FOR JAPAN, 27SEP-07OCT

From 9/27/14-10/07/14 Rene Sanchez and Jesson Hutchinson travelled to Japan. There were two main goals of this trip:

1. Participate in the PHYSOR conference in Kyoto.
2. Discuss future collaboration with JAEA and tour their experimental facilities.

This report mainly focuses on the PHYSOR conference, the JAEA tour was reported by Joetta Goda on 10/09/14 (attached to this trip report).

This year PHYSOR was held in Kyoto and had approximately 400 technical talks. Each presentation had a corresponding full paper. In our opinion, the quality of the papers at PHYSOR was very high. This trip report will focus on three areas of the PHYSOR conference: technical presentations, discussions for future collaboration, and updates on the Japanese nuclear industry since the March 11, 2011 tsunami and resulting accident at the Fukushima-Daiichi Nuclear Power Station.

As mentioned, there were approximately 400 technical talks. Rene and Jesson presented the following talks:

- Rene Sanchez, John Bounds, Todd Bredeweg, Joetta Goda, Travis Grove, David Hayes, Kevin Jackman, George Mckenzie, and William Myers, "Reaction Rate, Fission Product Yield, and Rossi-Alpha Measurements Using a HEU Metal, Copper Reflected Critical Assembly"
- J. Hutchinson, A. Sood, M. Smith-Nelson, J. Goda, J. Bounds, W. Myers, T. Cutler, B. Richard, B. Rooney, A. Chapelle, P. Casoli, N. Authier, "Caliban and Godiva-IV Measurements Using Helium-3 Detector Systems"

Both the full papers and slides from both of these talks are attached to this trip report. In addition, many of the technical talks are of particular interest to NCERC, LANL, and our sponsors. Below is a list of several of the most interesting talks. These can be obtained from Rene or Jesson upon request.

- **Brazil, Centro de Engenharia Nuclear:** A. Dos Santos, S. M. Lee, R. Jerez and R. Diniz , "THE EVALUATION OF THE SUBCRITICAL EXPERIMENTS PERFORMED IN THE IPEN/MB-01 RESEARCH REACTOR FACILITY FOR THE IRPhE PROJECT." This paper is a summary of the new subcritical benchmark in the 2014 ICSBEP handbook. More on this is discussed below.

Los Alamos
NATIONAL LABORATORY
EST 1943

memorandum

Nuclear Engineering and Nonproliferation Division

To/MS: David Hayes, NEN-2, B228
Thru/MS: William Myers, NEN-2, B228
From/MS: Jesson Hutchinson, NEN-2, B228
Rene Sanchez, NEN-2, B228
Phone/Email: 7-5411/jesson@lanl.gov

Symbol: NEN-2:14-39
Date: October 14, 2014

SUBJECT: TRIP REPORT FOR JAPAN, 27SEP-07OCT

From 9/27/14-10/07/14 Rene Sanchez and Jesson Hutchinson travelled to Japan. There were two main goals of this trip:

1. Participate in the PHYSOR conference in Kyoto.
2. Discuss future collaboration with JAEA and tour their experimental facilities.

This report mainly focuses on the PHYSOR conference, the JAEA tour was reported by Joetta Goda on 10/09/14 (attached to this trip report).

This year PHYSOR was held in Kyoto and had approximately 400 technical talks. Each presentation had a corresponding full paper. In our opinion, the quality of the papers at PHYSOR was very high. This trip report will focus on three areas of the PHYSOR conference: technical presentations, discussions for future collaboration, and updates on the Japanese nuclear industry since the March 11, 2011 tsunami and resulting accident at the Fukushima-Daiichi Nuclear Power Station.

As mentioned, there were approximately 400 technical talks. Rene and Jesson presented the following talks:

- Rene Sanchez, John Bounds, Todd Bredeweg, Joetta Goda, Travis Grove, David Hayes, Kevin Jackman, George Mckenzie, and William Myers, "Reaction Rate, Fission Product Yield, and Rossi-Alpha Measurements Using a HEU Metal, Copper Reflected Critical Assembly"
- J. Hutchinson, A. Sood, M. Smith-Nelson, J. Goda, J. Bounds, W. Myers, T. Cutler, B. Richard, B. Rooney, A. Chapelle, P. Casoli, N. Authier, "Caliban and Godiva-IV Measurements Using Helium-3 Detector Systems"

Both the full papers and slides from both of these talks are attached to this trip report. In addition, many of the technical talks are of particular interest to NCERC, LANL, and our sponsors. Below is a list of several of the most interesting talks. These can be obtained from Rene or Jesson upon request.

- **Brazil, Centro de Engenharia Nuclear:** A. Dos Santos, S. M. Lee, R. Jerez and R. Diniz , "THE EVALUATION OF THE SUBCRITICAL EXPERIMENTS PERFORMED IN THE IPEN/MB-01 RESEARCH REACTOR FACILITY FOR THE IRPhE PROJECT." This paper is a summary of the new subcritical benchmark in the 2014 ICSBEP handbook. More on this is discussed below.

- **Slovenia, Jozef Stefan Institute:** Luka Snoj presented two papers that were very interesting. The first was on installing a LiD DT thermal to 14 MeV neutron convertor in the TRIGA reactor at JSI. The second was on an impressive training program using the same TRIGA. Additional discussion with Luka is described below.
- **Belgium (and other countries):** Many talks (around ten) were given on the FREYA project. This project includes collaborations with several countries (Belgium, Italy, France, Germany, and possibly others). The majority of talks were on measurements on the VENUS-F core. These talks are of interest to NCERC because they relate to monitoring subcritical which is useful in both our subcritical measurements and critical experiment programs. Methods discussed included Rossi-alpha, source jerk, beam interruption, and others.
- **Japan, (Nagoya University and Kyoto University):** Several talks were given on measurements of the Kyoto University Critical Assembly (KUCA). These were of great interest to current subcritical neutron measurements.
- **Japan:** There was an entire session on research related to the Fukushima accident. Many papers focused on criticality safety of the fuel debris and are of great interest to the criticality safety community.
- **United States (LANL and University of Michigan):** A. Kaplin, et. al., "UTILIZING SIMULATED ROSSI-ALPHA DISTRIBUTIONS TO DEVELOP NEW METHODS OF CHARACTERIZING SPENT NUCLEAR FUEL." This paper is of interest because it uses techniques applicable to both critical and subcritical experiments.
- **Israel, Nuclear Research Center NEGEV:** E. Gilad, et. al., "ESTIMATION OF THE DELAYED NEUTRON FRACTION OF THE MAESTRO CORE IN MINERVE ZERO POWER REACTOR." This paper used oscillator measurements to determine the delayed neutron fraction. This is obviously of great interest to NCERC as we have tried to obtain an oscillator for future experiments (currently still unfunded).

Several productive discussions took place between the LANL personnel and staff from other organizations. Three of those are detailed below:

- Gregory Caplin, IRSN, France: At PHYSOR, we were able to continue discussions with Gregory on upcoming collaborations between IRSN and the US. Several topics were discussed and we will see Gregory again at the NCSP training course in January.
- Adimir Dos Santos, Centro de Engenharia Nuclear, Brazil: Adimir, a member of the ICSBEP working group, expressed interested in LANL helping with analysis of Feynman measurements on the IPEN/MB-01 research reactor (and possibly participating in future measurements).
- Luka Snoj, Jozef Stefan Institute, Slovenia: Luka, a member of the ICSBEP working group, expressed interest in possible future collaboration and measurements on their TRIGA reactor.

As mentioned above, the PHYSOR conference provided a great deal of information on Fukushima and the current state of the Japanese nuclear industry. While all of these details have likely been released, many of them have not been discussed very much in the US (to our knowledge). Below is a short list of things which were discussed. Note that this is our understanding of what was said, not the official stance of Japan:

- Following the accident, all nuclear power stations in Japan were shut down.
- In 2012 the Nuclear Regulation Authority was formed in Japan (the equivalent to the NRC). Until this time there was no oversight of nuclear plants in Japan.

- Based on work by the NRA, all plants are required to have increased safety measures. One location (with two reactors) has implemented all required measured and has a license to operate. Those plants operated in 2013-2014 but are currently shut down due to maintenance. Currently there are no operating nuclear plants in Japan. About half of the power plants in the country are working with the NRA and have submitted licenses to get back online.
- Due to Fukushima, all research reactors were also shut down. It is unclear if any of them are now operational again. STACY is being modified for experiments specifically aimed at helping with Fukushima efforts (there was a talk devoted to this at PHYSOR and at the ANS meeting in Reno last June).

Both the PHYSOR conference and JAEA meetings were very successful. This trip greatly benefitted LANL and the sponsors and future work will benefit from this trip (both in collaborations and research).

Attachments:
1. Sanchez full PHYSOR paper.
2. Sanchez PHYSOR slides.
3. Hutchinson PHYSOR paper.
4. Hutchinson PHYSOR slides.
5. Goda JAEA report.

Distribution: Joetta Goda, NEN-2, B228

PHYSOR 2014 – The Role of Reactor Physics Toward a Sustainable Future
The Westin Miyako, Kyoto, Japan, September 28 – October 3, 2014, on CD-ROM (2014)

Reaction Rate, Fission Product Yield, and Rossi-Alpha Measurements Using a HEU Metal, Copper Reflected Critical Assembly

Rene Sanchez[a], John Bounds[a], Todd Bredeweg[b], Joetta Goda[a], Travis Grove[a], David Hayes[a], Kevin Jackman[b], George Mckenzie[a], and William Myers[a]
[a]NEN-2: Advanced Nuclear Technology
[b]C-NR: Nuclear & Radiochemistry
Los Alamos National Laboratory
P. O. Box #1663 Los Alamos, New Mexico, 87544 USA
rsanchez@lanl.gov

ABSTRACT

A critical experiment was performed on the Comet assembly to provide nuclear data in a non-thermal neutron spectrum and to re-establish experimental measurement capabilities relevant to the United States Department of Energy's general purpose nuclear criticality experiments capability and to the Technical Nuclear Forensic program. Activation and fission foils were placed at specific locations in the Zeus all-oralloy core, copper reflected critical experiment to infer spectral indices data and obtain reaction rate data. After the irradiation, passive gamma ray measurements were performed on all the foils and several of them were packaged and shipped to Los Alamos National Laboratory for further radiochemical analysis. The results from the non-destructive and radiochemical analyses are presented. Finally, Rossi-α measurements were performed on a slightly modified configuration from the configuration used for the activation measurements. The Rossi-α results are presented and compared to past measurements performed using other critical assemblies.

Key Words: **Uranium, Critical experiments, Spectral indices, Rossi-α.**

1. INTRODUCTION

The National Criticality Experiments Research Center (NCERC) at the Nevada National Security Site (NNSS) is home to four assemblies for the use of conducting critical experiments. One of these assemblies is named Comet, which is a vertical-lift machine designed to support performance of experiments that are sub-critical or operate in the critical regime at delayed critical and above but below prompt critical. Comet was the second of four assemblies returned to service after the shutdown at TA-18 at the Los Alamos National Laboratory (LANL) in 2004.

In mid-2010, a configuration from the Zeus series of critical experiments was selected to be assembled on the Comet machine to support performance of a neutron irradiation experiment to activate twelve foils. A detailed description of this Zeus core is given below. The purpose of the experiment was to measure fission product activities, activation products (GA, Ir, Au), fission ratios, and the amount of ^{237}U created from ^{238}U(n, 2n). Additionally, these reactions were intended to help establish the foundation for performing future irradiations such as measuring reaction rates and fission-product yields. The results of the radiochemical destructive and non-destructive analyses of the six LANL foils are presented here as well as the inferred spectral indices. Rossi-α measurements were performed with the configuration at varying states of criticality (or values of K_{eff}) and the prompt-neutron decay constants were determined. Using these data, the Rossi-α values at delayed critical was inferred and the neutron lifetime for the configu-

ration was estimated.

2. DESCRIPTION OF THE EXPERIMENT

2.1. Zeus Configurations

The Zeus series of experiments consists of a cylindrical core region that is surrounded on all sides by a metallic copper reflector.[1] The core is divided into an upper portion and a lower portion. The upper portion rests on a thin, square stainless steel plate, called diaphragm, which is supported by the inner corner copper reflectors. The bottom portion of the core sits on the top of the bottom reflector. The bottom reflector, in turn, sits on the movable platen of the Comet vertical assembly machine as illustrated in Fig. 1. The lower portion of the core is held in position by a central, hollow aluminum alignment tube, the top of which is approximately 1/16-in below the top unit on the movable platen. Two resistance temperatures detectors (RTDs) are positioned inside the hollow aluminum alignment tube to measure the temperature increase during a high power run. The top, corner, and side reflectors rest on a stationary aluminum plate attached to the Comet machine.

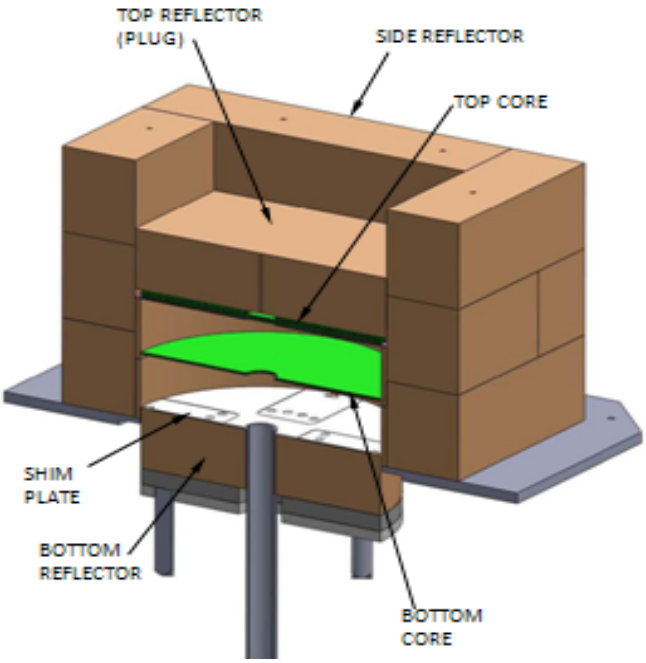

Figure 1. Final configuration showing the aluminum shims and the four trays where the irradiation foils were placed**.**

The experiment is assembled by raising the bottom portion of the assembly into a blind hole until it makes full contact with the steel diaphragm that supports the top portion of the core. For this irradiation, the top portion of the core contained six HEU metal units. The bottom portion of the core contained two HEU metal units plus a 1/8-in thick aluminum metal shim. The aluminum metal shim was designed to have four aluminum metal trays with circular cavities machined where the irradiation foils were placed. A thin aluminum metal foil was placed over the cavities openings containing the irradiation foils to minimize the chance of cross contamination with the HEU metal unit that resided above. The trays were designed to slide out and away from the shim without having to remove units stacked above. The aluminum shim with its four aluminum trays containing irradiation foils was placed between the bottom copper reflector and the bottom HEU metal unit as illustrated in Fig. 1.

For the Rossi-α measurements, the core was re-configured so that the top portion of the core contained four HEU units plus a smaller 6-in in diameter HEU plate. The bottom portion of the core contained four HEU units plus 0.0185-in aluminum shims and an interlocking aluminum sample plate. In both cases, each HEU metal unit used in these experiments had two components, an inner disk and an outer ring.

For the irradiation foil experiment, the inner disks in the bottom portion of the core and the top two inner disks in the top portion of the core have a 2.50-in diameter hole to accommodate the alignment tube. In contrast, the four remaining inner disks in the top portion of the core are solid plates of HEU metal.

For both experiments, the HEU plates are approximately 0.118-in thick and the solid disks are 15-in in diameter. The inner disks with central holes are 15-in OD and 2.5-in ID. The outer rings are approximately 21-in OD and 15-in ID. Table 1 and 2 show the weights and part numbers of each of the plates used in these experiments. The uranium metal plates are on average 93.22 wt% ^{235}U, and 5.67 wt% ^{238}U with an average density of 18.8 g/cc.

Table 1. Description of uranium plates and their weights as loaded on the assembly for the foil irradiation.

Upper Portion of the Core					
Part Number	**Description**	**Weight (g)**	**Part Number**	**Description**	**Weight (g)**
B-2444-01	Outer Ring 21-in OD 15-in ID	6122.4	10464	Inner Disk 15-in OD 2.5-in ID	6259.2
B-2444-02	Outer Ring 21-in OD 15-in ID	6131.2	10475	Inner Disk 15-in OD 2.5-in ID	6235.8
B-2444-13	Outer Ring 21-in OD 15-in ID	6027.7	11017	Inner Disk 15-in Diameter Solid Plate	6516.8
B-2444-19	Outer Ring 21-in OD 15-in ID	6135.0	11149	Inner Disk 15-in Diameter Solid Plate	6405.4
B-2444-10	Outer Ring 21-in OD 15-in ID	6137.7	11147	Inner Disk 15-in Diameter Solid Plate	6523.6
B-2444-27	Outer Ring 21-in OD 15-in ID	6074.7	11150	Inner Disk 15-in Diameter Solid Plate	6429.2
Bottom Portion of the Core					
B-2444-33	Outer Ring 21-in OD 15-in ID	6158.6	10491	Inner Disk 15-in OD 2.5-in ID	6391.7
B-2444-29	Outer Ring 21-in OD 15-in ID	6131.7	10467	Inner Disk 15-in OD 2.5-in ID	6336.4
1/8-in Thick Aluminum Shim					
Total Uranium Mass 100,017.1 g					

As mentioned above, the reflector pieces are made of metallic copper and they are arranged as shown in Fig. 1. The copper top reflector is a parallelepiped 22-in square and 5.678-in in height weighing approximately 880 lbs. The copper bottom reflector is a short fat cylinder with a 21-in OD, 2.5-in ID, and 5.68-in height. The bottom reflector weighs approximately 627 lbs. The side reflectors are parallelepipeds 8.13-in by 6.38-in by 28.38-in weighing approximately 476 lbs each. There are also copper corner pieces of different heights that are placed inside the side reflectors to be able to go from a square blind hole to a circular blind hole. There is a 0.050-in air gap between

the fuel and the side reflector.

Table 2. Description of uranium plates and their weights as loaded on the assembly for the Rossi-α measurements.

Upper Portion of the Core					
Part Number	Description	Weight (g)	Part Number	Description	Weight (g)
-	-	-	10475	Inner Disk 6-in Diameter Solid Plate	1077.3
B-2444-13	Outer Ring 21-in OD 15-in ID	6027.2	11017	Inner Disk 15-in Diameter Solid Plate	6515.9
B-2444-19	Outer Ring 21-in OD 15-in ID	6135.6	11149	Inner Disk 15-in Diameter Solid Plate	6406.4
B-2444-10	Outer Ring 21-in OD 15-in ID	6136.9	11147	Inner Disk 15-in Diameter Solid Plate	6522.6
B-2444-27	Outer Ring 21-in OD 15-in ID	6073.7	11150	Inner Disk 15-in Diameter Solid Plate	6428.6
Bottom Portion of the Core					
Interlocking Aluminum Sample Plate					
0.0185-inch thick aluminum shims					
B-2444-01	Outer Ring 21-in OD 15-in ID	6122.8	10464	Inner Disk 15-in OD 2.5-in ID	6259.1
B-2444-02	Outer Ring 21-in OD 15-in ID	6131.1	10475	Inner Disk 15-in OD 2.5-in ID	6236.8
B-2444-31	Outer Ring 21-in OD 15-in ID	6173.8	10491	Inner Disk 15-in OD 2.5-in ID	6391.7
B-2444-33	Outer Ring 21-in OD 15-in ID	6159.4	10489	Inner Disk 15-in OD 2.5-in ID	6344.8
Total Uranium Mass 101,143.1 g					

2.2. Irradiations

The experiment was designed to have twelve foils irradiated in locations equidistant from the core axis. This required the insertion of a 1/8-in thick aluminum shim into the assembly where foils could be placed and easily recovered.[2] Four of these foils were measured, packaged, and shipped to Pacific Northwest National Laboratory (PNNL) for further analysis and the results from their analysis are not discussed in this paper. The remainder eight foils belonged to LANL. One of the irradiation sample trays loaded with LANL foils is shown in Fig. 2.

After the irradiation, six of the eight LANL foils were measured in the NCERC counting room, packaged, and shipped to LANL TA-48 for further analysis. Four of the six foils were chemically dissolved and destructive analysis was performed on them. The final two foils were measured and remained at NCERC for future reuse. The configurations of the four trays are described below.

Tray 1 (PNNL)
Tray 2 (/NCERC/LANL):
NCERC:
Depleted Uranium (DU) foil D-38-10-7, 0.5806 grams

HEU foil 8551-410, 0.0637 grams
LANL:
Au foil 11A, 0.1273 grams (sample ID 4116)
Pu foil JX-2229-D5, 0.3899 grams (Ni clad) (sample ID 4113)
Tray 3 (LANL);
HEU foil8551-408, 0.0638 grams (sample ID 4111)
DU foil D-38-10-5, 0.5803 grams (sample ID 4112)
Gallium (Ga) sample, 0.06087 grams of Ga_2O_3 (sample ID 4114)
Iridium (Ir) sample, 0.10745 grams of K_2IrCl_6 (sample ID 4115)
Tray 4 (Empty)

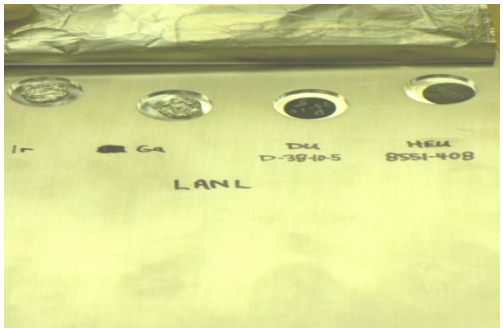

Figure 2. Foils Loaded in Tray Prior to Irradiation.

The Comet assembly with the ZEUS configuration described above was run at an average power of about 2.3 kW on September 8, 2011 for 3,955 seconds as measured on the linear channel #2. The zero time (ZT) corresponding to the end of bombardment (EOB) was 251.95 GMT in Julian day decimal time. The foils were recovered late in the morning of September 12, 2011 (. During the recovery, the irradiation foils were placed on aluminum sample plates and cover with thin Mylar.

2.2.1 Radiochemistry

Most of the foils arrived at LANL, on September 20, 2011 and were delivered to TA-48. The irradiated ^{239}Pu sample arrived on the afternoon of Wednesday, September 21, 2011. The foils were given initial gamma-ray counts on High Purity Germanium (HPGe) detectors while still on the original sample plates. It was decided that the Pu, HEU, and DU samples would be dissolved. On September 21, 2011, the two uranium foils were removed from their mounts by cutting away the Mylar and dropping the foils into 600 mL Teflon beakers for dissolution. The uranium foils were dissolved using concentrated HNO_3 and HCL. A small amount of fuming HNO_3 was needed to complete the dissolution due to small amount of oxide that had formed on the foils. The resulting solutions were diluted to approximately 100 mL in 4 M HNO_3 in 125 mL Teflon bottles. 5 mL aliquots of the “A” solutions were prepared and delivered to the count room for gamma spectroscopy. The 5 mL aliquots were gamma counted on HPGe detectors for a week. 80 mL aliquots were prepared for the sequential separation and the separation process was completed on Thursday, September 22.

The nickel-clad plutonium foil was placed into a 600 ml Teflon beaker for dissolution. The nickel coating was dissolved using 6 M HCL at approximately 200 . The plutonium foil was then dissolved using concentrated HNO_3, fuming HNO_3, and HF at 280 . The resulting solution was concentrated to near dryness and brought up in a 100 mL of 4 M HNO_3 in a Teflon bottle. A 5 mL

aliquot of the resulting "A" solution was prepared for gamma assay and an 80 mL aliquot was prepared for the sequential separation.

The whole "A" solution aliquots were analyzed for several fission products (^{99}Mo, ^{99m}Tc, ^{95}Zr, ^{103}Ru, ^{132}Te, ^{140}Ba, ^{141}Ce, ^{147}Nd) using gamma spectroscopy. The 10-element plus lanthanides sequential separation provided fractions for purification including Ba/Sr, Zr, Mo, Cs, Ag, Cd, Sm, Eu, Tb, U, Np, and Pu. From these sequential fractions, separated samples of Mo, Ag, Sm, Eu, and Np were prepared and counted for the ^{235}U foil experiment, 4111. From the sequential fractions in the ^{238}U experiment (4112), separated samples of Mo, Ag, Sm, Eu, and Tb were prepared and counted. Finally, from the sequential fractions in the ^{239}Pu experiment (4113), separated samples of Mo, Ag, Sm, Eu, and Tb were prepared and counted. Molybdenum was further purified and mounted as MoO_3.

The separated samples were beta and gamma counted for the fission products and actinides. The isotopics of the uranium foils (4111, and 4112) were analyzed using inductive-coupled plasma mass spectrometry (ICP-MS). The iridium foil was also chemically dissolved, separated, and analyzed using a combination of gamma spectroscopy and x-ray counting. The gold and gallium foils were only measured by gamma spectroscopy. The results are corrected for decay during counting and irradiation. However, the values are not corrected for gamma-ray self-absorption or summing effects. The results for the PNNL and NCERC foils are not presented in this paper.

3. EXPERIMENTAL RESULTS

3.1. Gold (4116)

The gold foil, serial number 11A, had a mass of 0.1273 grams. Gold is often used as an activation foil because of the large neutron capture cross section of ^{197}Au. Gold also has a high absorption resonance at 5 eV, and can be used in conjunction with Cd covered gold foil to estimate the thermal flux. Unfortunately, the Cd covered Au foil was not included for the irradiation. The gold foil was measured using gamma spectroscopy at LANL, and the only isotopes of gold observed were ^{196}Au and ^{198}Au. Table 3 shows the determined activities and atoms per gram of foil. The values reported are the average of four separate measurements made on different gamma-ray counting systems.

Table 3. Measured activities and atoms per gram of foil for gold isotopes.

Isotope	DPM @ EOB	Atoms/g foil @ EOB
^{196}Au	2.51E+04 ± 7.8%	2.53E+09 ± 7.8%
^{198}Au	1.08E+07 ± 4.3%	4.76E+11 ± 4.3%

3.2. Iridium (4115)

The iridium foil consisted of 0.10745 grams of K_2IrCl_6 wrapped in aluminum foil. The K_2IrCl_6 was dissolved and the iridium was chemically separated using a procedure outlined in LA-1721.[3] The isotopes ^{189}Ir, ^{190}Ir, and ^{192}Ir were determined by gamma counting, and ^{192m}Ir was determined by X-ray counting. The iridium results are shown in Table 4. The value for ^{189}Ir is reported as the estimated upper limit for what the measurement instrument could observe. The values reported per gram of precipitated sample because there is no equivalent "A" solution for the iridium chemistry.

3.3. Gallium (4114)

The gallium foil consisted of 0.06087grams of Ga_2O_3 wrapped in aluminum foil. ^{72}Ga was the only isotope measured because of the other gallium isotopes had short half-lives relative to the recovery

Table 4. Atoms per gram of foil for iridium isotopes.

Isotope	Atoms/g foil @ EOB
^{189}Ir	7E+06 (Limit)
^{190}Ir	8.7E+08 ± 50.3%
^{192}Ir	1.233E+11 ± 0.18%
^{193m}Ir	6.76E+10 ± 0.70 %

time. Table 5 shows the results from the gamma spectroscopy measurements at NCERC. It should be noted that the uncertainties on the measurement are quite high because the counting statistics were low and the lack of the appropriate calibration curve for the counting geometry. The efficiency curve for this counting geometry was estimated using the KMESS code.[4]

Table 5. Measure activity and atoms per gram of foil for gallium.

Isotope	DPM @ EOB	Atoms/g foil @ EOB
Ga-72	2.4E+04 ± 21%	4.8E+08 ± 21%

3.4. Plutonium (4113)

The plutonium foil, serial number JX-2229-D5 (nickel clad), had a mass of 0.3899 grams, and was dissolved into an "A" solution with a total mass of 119.074 grams. The separated fission products were measured by gas-flow proportional β-counters. The β-counting estimated number of fissions per gram of "A" solution based on the ^{99}Mo is 1.21E+10 ± 0.3%, and the total number of fissions is 1.44E+12 ± 0.3%. The cumulative fission chain yield used in this conversion was for thermal fission in ^{235}U of ^{99}Mo, namely 6.11%.[5] For comparison, the cumulative fission chain yield for fast fission in ^{239}Pu of ^{99}Mo is 5.98%.[5] The actinide composition of the plutonium foil was not analyzed.

3.5. Depleted Uranium (4112)

The DU foil, serial number D-38-10-5, had a mass of 0.5803 grams, and was dissolved into an "A" solution with a total mass of 116.679 grams. The separated fission products were also measured by gas-flow proportional β-counters. The β-counting estimated number of fissions per gram of "A" solution based on the ^{99}Mo is 1.29E+09 ± 0.3%, and the total number of fissions is 1.505e+11 ± 0.3%. The cumulative fission chain yield used in this conversion was also for thermal fission in ^{235}U of ^{99}Mo. Again, for comparison, the cumulative fission yield for fast fission in ^{238}U of ^{99}Mo is 6.17%.[5] The uranium composition was also analyzed using ICP-MS. The isotopic composition of the DU foil is shown in Table 6. Notice the amount of ^{238}U is greater than in natural uranium (99.3%) as expected.

Table 6. Uranium composition of the DU foil.

Isotope	Composition (%)
^{234}U	1.1E-04 ± 17.8%
^{235}U	2.63E-01 ± 1.5%
^{236}U	2.8E-03 ± 10.7%
^{238}U	9.9733E+01 ± 0.004%

3.6. Highly-Enriched Uranium (4111)

The HEU foil, serial number 8551-408, had a mass of 0.0638 grams, and was dissolved into an "A" solution with a total mass of 116.166 grams. The separated fission products were also measured by gas-flow proportional β-counters. The β-counting estimated number of fissions per gram of "A" solution based on ^{99}Mo is 1.423E+09 ± 0.2%, and the total number of fissions is 1.653E+11 ± 0.2%. The cumulative fission chain yield used in this conversion was also for thermal fission in ^{235}U of ^{99}Mo. Again, for comparison, the cumulative fission yield for fast fission in ^{235}U of ^{99}Mo is 5.94%.[5] The uranium composition of the HEU foil was also analyzed using ICP-MS. The isotopic composition of the uranium foil is shown in Table 7. Notice that the enrichment appears to be about 93.2% which is consistent with HEU.

Table 7. Uranium composition of the HEU foil.

Isotope	Composition (%)
^{234}U	8.92E-01 ± 0.7%
^{235}U	9.324E+01 ± 0.03%
^{236}U	5.57E-01 ± 1.2%
^{238}U	5.31E+00 ± 0.5%

3.6. Spectral Indices (Fission Ratios)

Fission ratios are important because they provide information regarding the neutron spectrum for a particular experiment. To determine these ratios, the information provided in the previous sections is used.

For the DU foil, the fissions per gram of "A" solution is reported as 1.29E+09 and the mass of the solution (that includes the entire DU foil) was 116.679 grams, so the total fissions for the entire DU foil dissolved in "A" solution were 1.505E+11. The mass of the DU foil was reported as 0.5803 grams and using 99.733 % ^{238}U by weight, the fissions per gram of ^{238}U were 1.505E+11/(0.5803*0.99733)=2.60E+11. There are 0.00252973E+24 atoms ^{238}U atoms/(g ^{238}U), so the fissions/(atom ^{238}U) is 2.60E+11 fissions/(g ^{238}U)/(0.00252973E+24 atoms/(g ^{238}U)) = 1.027E+14 fissions/(10E+24 atoms ^{238}U).

For the HEU foil, the fissions per gram of "A" solution reported as 1.423E+09 and the mass of solution "A" (That includes the HEU foil) was 116.166 grams, so the total number of fissions for the entire HEU foil dissolved in "A" solution were 1.653E+11. The mass of the HEU foil was reported as 0.0638 grams and using an enrichment of 93.24% ^{235}U by weight, the fissions per gram of ^{235}U were 1.653E+11/(0.0638*0.9324) = 2.779E+12. There are 0.00256209E+24 atoms ^{235}U/(g ^{235}U) so the fissions/(atom ^{235}U) is 2.779E+12 fissions/(g ^{235}U)/(0.00256209E+24 atoms ^{235}U/(g

^{235}U)) = 1.085E+15 fissions/(10E+24 atoms ^{235}U).

Finally, for the Pu foil, the fissions per gram of “A” solution is reported as 1.21E+10 and the mass of solution “A” (that includes the entire Pu foil) was 119.074 grams, so the total fissions for the entire PU foil dissolved in “A” solution were 1.44E+12. The mass of the Pu foil was reported as 0.3899 grams and using an enrichment of 95.82% ^{239}Pu by weight, the fissions per gram of ^{239}Pu were 1.44E+12/(0.3899*0.9582)=3.854E+12. There are 0.0025192E+24 atoms ^{239}Pu/(g ^{239}Pu) so the fissions/(atom ^{239}Pu) is 3.854E+12 fissions/(g ^{239}Pu)/0.0025192E+24 atoms ^{239}Pu/(g ^{239}Pu) = 1.530EE+15 fissions/(10E+24 atoms ^{239}Pu).

As stated in the previous sections, the thermal fission yield of ^{235}U was used to covert to count rates from ^{99}Mo to fission rates. Because this critical experiment is a fast system, fast fission yields should be used with the appropriate fission foil. Thus, the total fissions per gram were estimated based on the ^{99}Mo activity and the fast fission yields of 6.17% for ^{238}U, 5.94% for ^{235}U, and 5.98% for ^{239}Pu.[5]

For the DU foil, the fission per gram of ^{238}U given the new conversion factor is 2.60E+11*0.0611/0.0617 = 2.57E+11. The fissions per atom of ^{238}U is 1.027E+14 fissions/(10E+24 atoms ^{238}U) *0.0611/0.0617 = 1.017E+14/(10E+24 atoms ^{238}U).

For the HEU foil, the fissions per gram of ^{235}U given the new conversion factor is 2.77E+12*0.0611/0.0594 = 2.859E+12. The fissions per atom of ^{235}U is 1.085E+15 fissions/(10E+24 atoms ^{235}U)*0.0611/0.0594 =1.116E+15/(10E+24 atoms ^{235}U).

Uranium oxide is 88% uranium by weight. Since the uranium foils are bare, they have some oxidation on their surfaces. The 0.0638 grams reported for the HEU foil and the 0.5803 grams reported for the DU foil were historic values of the masses. The foils could have been heavier from oxidation or lighter from flaking off of material. The foils that were irradiated were not weighed before they were dissolved, so their masses are not known precisely. The computed values for the fissions/(g ^{235}U or ^{238}U) discussed above assumed that the reported foil masses were correct.

Finally, for the Pu foil, the fissions per gram of ^{239}Pu given the new conversion factor is 3.854e+12*0.0611/0.0598 = 3.937E+12. The fissions per atom of ^{239}Pu is 1.530E+15fissions/(10E+24 atoms ^{239}Pu)*0.0611/0.0598 =1.563E+15/(10E+24 atoms ^{239}Pu).

The total fissions per gram and fissions per atom per atom of each of the fission foils are presented in Table 8. Additionally, the observed fission ratios (spectral indices) for the experiment and other critical assemblies are shown in the same table.[6, 7]

The Godiva-I[8] assembly, also known as Lady Godiva, was a bare 94% enriched ^{235}U metal spherical critical assembly. It is expected that the neutron spectrum in this assembly approaches that of a pure ^{235}U fission spectrum. On the other hand, Topsy[9] was an assembly with a pseudo-spherical 94% ^{235}U metal core surrounded by a thick natural uranium reflector. For the Topsy assembly, the neutron spectrum was slightly softer when compared to Lady Godiva because the reflected neutrons would have slightly less energy than those neutrons produced during the fission process. For the Zeus all-oralloy core, the neutron spectrum should be the softest of the three because the neutrons reflected back from the copper reflector would have less energy than those reflected back from natural uranium. As seen in Table 8, the and ratios are the lowest for the Lady Godiva assembly followed by Topsy and the Zeus all-oralloy experiment, which confirm our assumptions stated above.

3.7. Rossi-α Measurements

Rossi-α measurements were performed on the Zeus all-oralloy experiment described above to determine the prompt neutron decay constants. These constants represent an eigenvalue characteristic of these particular assemblies, which can be experimentally measured by the Rossi-α or the pulse neutron source techniques and calculated by a deterministic or Monte Carlo method. In the

Table 8. Total fissions/gram, fissions/atom, and fission ratios.

Zeus all oralloy experiment						
Total number of fissions/gram						
^{235}U		^{238}U			^{239}Pu	
2.575E+11		2.859E+12			3.937E+12	
Total number of fissions/(10E+24 atoms)						
^{235}U		^{238}U			^{239}Pu	
1.017E+14		1.116E+15			1.563E+15	
Critical Assembly	— ———		— ———		— ———	
Zeus all oralloy	11.10 mass basis	10.97 atom basis	1.38 mass basis	1.40 atom basis	15.29 mass basis	15.37 Atom basis
Godiva-I Bare Oy-94	6.5 mass basis	-	1.42 mass basis	-	9.23 mass basis	-
Topsy (Oy-94 in thick NU)	7.3 mass basis	-	1.40 mass basis	-	10.22	-

measurements presented in this paper, the Zeus all-oralloy experiment was assembled to a high subcritcal neutron multiplication and the prompt neutron decay constants were obtained by the Rossi-α technique described in Ref. 10.

The critical experiment where the Rossi-α measurements were performed is described in section 2.1. Table 2 describes the configuration that was used for the Rossi-α measurements. Four bare ^{3}He detectors approximately 0.64 cm in diameter and 7.62 cm in length were placed inside the aluminum alignment tube (see Fig. 3) to measure the prompt neutron decay constants. Each detector had a standard fill pressure of 40-atmospheres of ^{3}He so that detectors could provide high neutron sensitivity despite their small size.

Rossi-α measurements were performed at several separation distances between the upper portion and lower portion of the Zeus core. The data were collected using a list- mode data acquisition module. This module has the capability of recording temporal information (relative to some reference starting time) and channel number for individual detection events with a time resolution of up to 100 nanoseconds. A program was written using Mathematica to sort each pulse according to their time of arrival into a time window containing 10,000 time bins, each bin being one microsecond wide. The stored data can be analyzed using different size of time bins without having to repeat the experiment. A least squares fit using the equation $f(t) = Ae^{-\alpha t} + C$ was performed for the binned data measured at each separation distance to determine the best value for alpha (see Fig. 4).

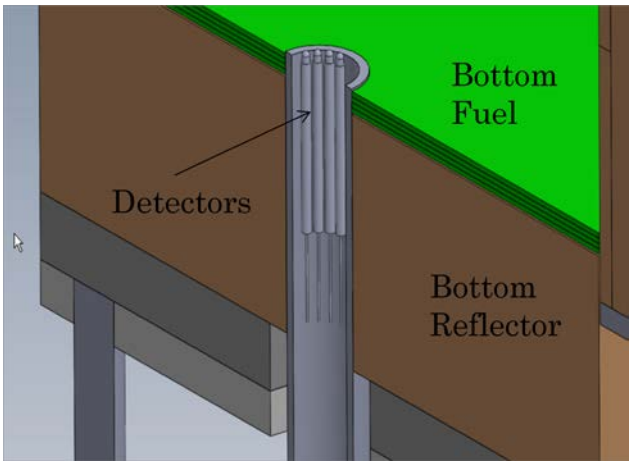

Figure 3. Final configuration showing the four bare ^{3}He detectors inside the aluminum alignment tube.

The prompt neutron decay constant at delayed critical was obtained by plotting the alphas at a particular subcritical separation distance as a function of inverse count rate and extrapolating linearly to an inverse count rate of zero (see Fig. 5).

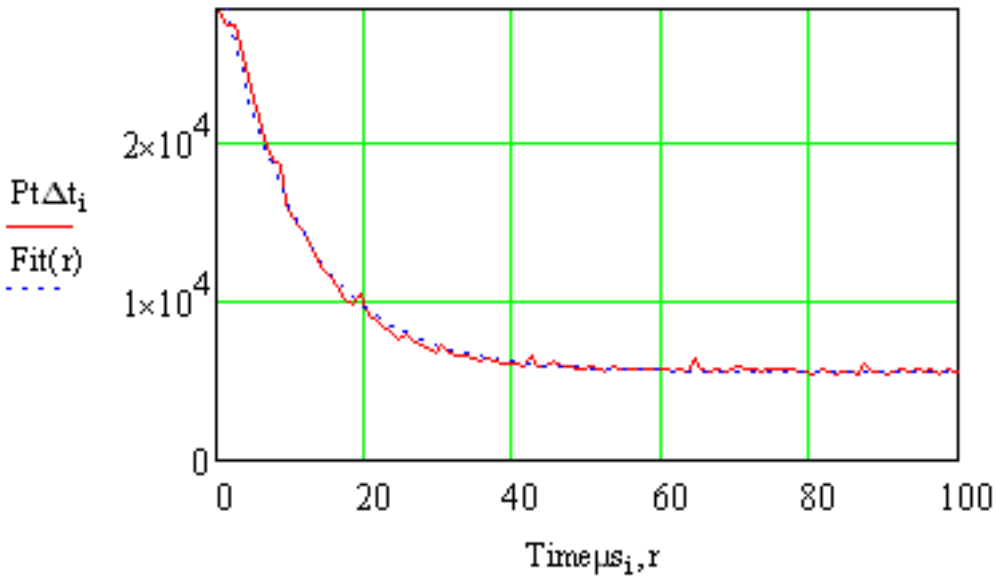

Figure 4. Least square fit of the binned data.

From Figure 5, the delayed critical prompt decay constant for this Zeus configuration is -82,694 ± 1073 sec^{-1}. Note the R^2 value of 1 indicating a perfect fit for the three points on the graph. The alpha at delayed critical obtained for this experiment compares quite well with other alpha values from other critical experiments. Table 9 shows a comparison of the alphas at delayed critical for different assemblies. Using an assumed effective delayed neutron fraction (denoted as β_{eff}) based on the type of fuel and the values of alpha from Table 9 above, the neutron lifetimes can be calculated and compared to the expected results. As mentioned in section 3.6, Lady Godiva is expected to have the hardest neutron spectrum and the shortest neutron lifetime.

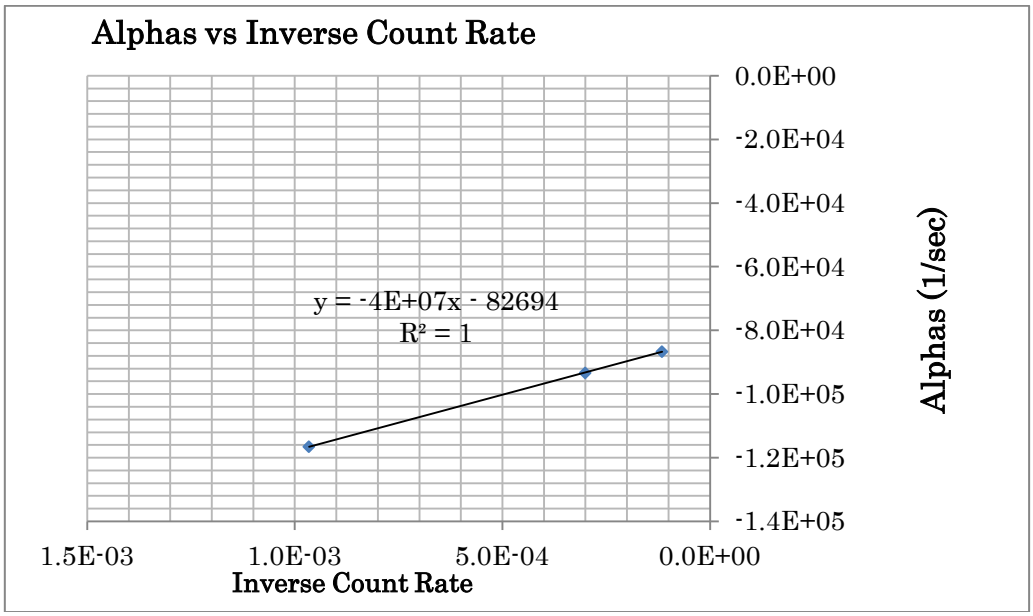

Figure 5. Alphas as a function of inverse count rate.

Table 9. Rossi-α at delayed critical for different assemblies.

Assembly	$\alpha_{dc}(sec^{-1})$
Lady Godiva (bare Oy-94)[6]	**-1.1×10^6**
Godiva IV (bare Oy-94 with 1.5 wt% Mo)[a]	**-0.84×10^6**
Topsy (Oy-94 in thick Natural Uranium)[6]	**-0.37×10^6**
Zeus all-oralloy experiment[a]	**-0.82694×10^5**
SHEBA II(solution assembly)[a]	**200**

[a]Measured values.

Assuming a β_{eff} value of 0.0065 for Lady Godiva and $\alpha_{dc} = \beta_{eff}/l$ where l denotes the neutron lifetime, we obtain a neutron lifetime of 5.9×10^{-9} seconds. It is expected that for the most recent assembly in the Godiva series (Godiva IV), the neutron spectrum is softer due to the presence of 1.5 wt% Mo that is part of the uranium alloy that constitutes the fuel material. The neutron lifetime for this assembly based on a β_{eff} of 0.0065 is 7.7×10^{-9} seconds, which confirms our expectations. For the Topsy assembly, the neutron spectrum should be softer when compared to either of the two Godiva assemblies because the contribution from reflected neutrons caused by the natural uranium reflector would have slightly less energy than those prompt neutrons produced during the fission process. Again, based on a β_{eff} value of 0.0065, the neutron lifetime for the Topsy assembly is 1.75×10^{-8} seconds, which is a longer neutron lifetime when compared with the previous assemblies. For this Zeus configuration, based upon the measured Rossi-α data at delayed critical and using a β_{eff} value of 0.0065, the neutron lifetime is 7.86×10^{-8}seconds. As expected, the neutron spectrum for this experiment is indicated to be softer than the Godiva series assemblies and the Topsy assembly. This is due to differences in reflection properties of copper versus natural uranium versus not having a reflector present. Finally, SHEBA II was a bare, uranyl fluoride, 4.5 wt% enriched ^{235}U solution assembly. Using the value for Rossi-α at delayed critical given in Table 9 and using a calculated β_{eff} value of 0.0080, the neutron lifetime for the SHEBA II assembly is 40×10^{-6} seconds, which is the softest of all the assemblies shown in Table 9.

5. CONCLUSIONS

Excellent results were achieved from the irradiation of foils and subsequent radiochemical analyses for this experiment. Spectral indices data were determined based on the non-destructive and radiochemical analysis estimates for fissions induced on the fissionable and fissile foils. The results from these measurements agreed as expected when compared with historical data obtained from past critical experiments. Finally, Rossi-α measurements were performed on this Zeus configuration and the results from these measurements were compared with results from other assemblies. Again, the Rossi-α data from this measurement campaign agreed as expected when compared to other critical experiments.

ACKNOWLEDGMENTS

The authors would like to thank the following people for their support and commitment in this research project: Robert Little, Tim Beller, Bill Haag, Theresa Cutler, Eric Sorensen, Christopher Romero, George Brooks, Mike MacInnes, Don Dry, Michael Gallegos, Michael Cisneros, and Rowena Gibson.

This work was supported in part by the DOE Nuclear Criticality Safety Program, funded and managed by the National Nuclear Security Administration for the Department of Energy.

REFERENCES

[1] R. D. Mosteller, “The Unmoderated Zeus Experiment: A Cylindrical HEU Core Surrounded by a Copper Reflector,” HEU-MET-FAST-073, in “International Handbook of Evaluated Criticality Safety Benchmark Experiments,” NEA/NSC/DOC (95) 03, Nuclear Energy Agency, Organisation for Economic Co-operation and Development (Sep. 2009).

[2] W. L. Myers, J. A. Bounds, and R. G. Sanchez, “IER-163: Reaction Rate and Fission-Product Yield Measurements with the Comet Assembly CEDT Phase-1 Detailed Plan,” Los Alamos National Laboratory report, LA-UR-11-05723, 2011.

[3] J. Kleinberg, “Collected Radiochemical and Geochemical Procedures,” Fifth Edition, Los Alamos National Laboratory report, LA-1721, 1990.

[4] K. R. Jackman, “KMESS: An Open-Source Software Package Using a Semi-empirical Mesh-Grid Method for the Modeling of Germanium Detector Efficiencies,” Ph. D. Dissertation, The University of Texas at Austin, 2007.

[5] T. R. England and B. F. Rider, “ENDF/349: Evaluation and Compilation of Fission Product Yields 1993,” Los Alamos National Laboratory, LA-UR-94-3106, ENDF-349, 1993.

[6] L. J. Koch and H. C. Paxton, “Fast Reactors,” Annual Review of Nuclear Science, Vol. 9, 1959.

[7] G. E. Hansen, “Status of Computational and Experimental Correlations for Los Alamos Fast-Neutron Critical Assemblies,” Physics of Fast and Intermediate Reactors, 1, 445-455, IAEA, Vienna (1962).

[8] R. E. Peterson, “Lady Godiva: An Unreflected ^{235}U Critical Assembly,” Los Alamos National Laboratory report LA-1614, September, 1953.

[9] R. H. White, “Topsy: A Remotely Controlled Machine for the Study of Critical Assemblies,” Los Alamos National Laboratory LA-1579, June, 1953.

[10] J. Ordoff, “Prompt Neutron Periods of Metal Critical Assemblies,” Nucl. Sci. & Eng., **2**, 450 (1957).

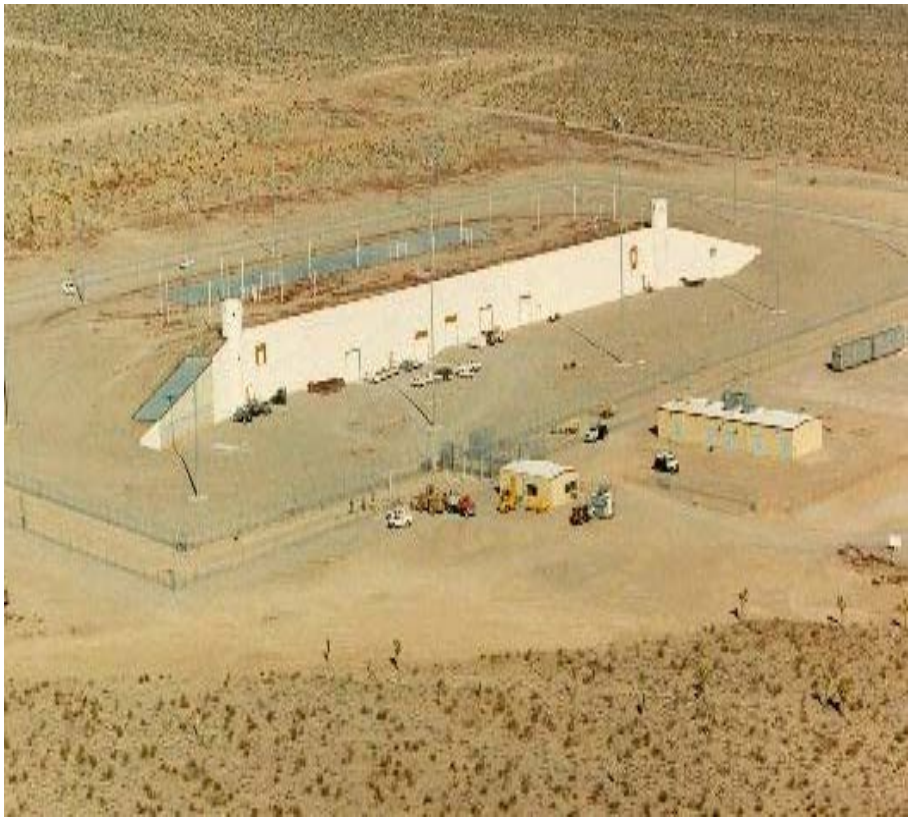

Reaction Rate, Fission Product Yield, and Rossi-α Measurements Using a HEU Metal, Copper Reflected Critical Assembly.

Rene Sanchez, John Bounds, Todd Bredeweg, Joetta Goda, Travis Grove, David Hayes, Kevin Jackman, George Mckenzie, and William Myers

National Nuclear Security Administration

Los Alamos NATIONAL LABORATORY

Background

- **Re-establish experimental measurement capability**
  - 1946-2004 Los Alamos Critical Experiments Facility (LACEF)
  - 2004-20011 LACEF moves to DAF at NTS (NCERC)
- **In Mid-2010, a configuration from the Zeus/Comet series of critical experiments**
  - August-September 2011
- **Re-establish the technical capability of the Nuclear Forensic program**

Purpose

- **Comet Startup**

Purpose:

To perform a critical experiment, Zeus, which is intended to benchmark ^{235}U cross sections in a variable energy spectrum.

To provide nuclear data in a non-thermal neutron spectrum that is relevant to the Stockpile Stewardship and Nuclear Forensic programs

Calculations (MCNP)

Reference
C. Wilkerson, Memo to W. Myers
"Zeus/Comet Irradiation," Aug 1, 2011

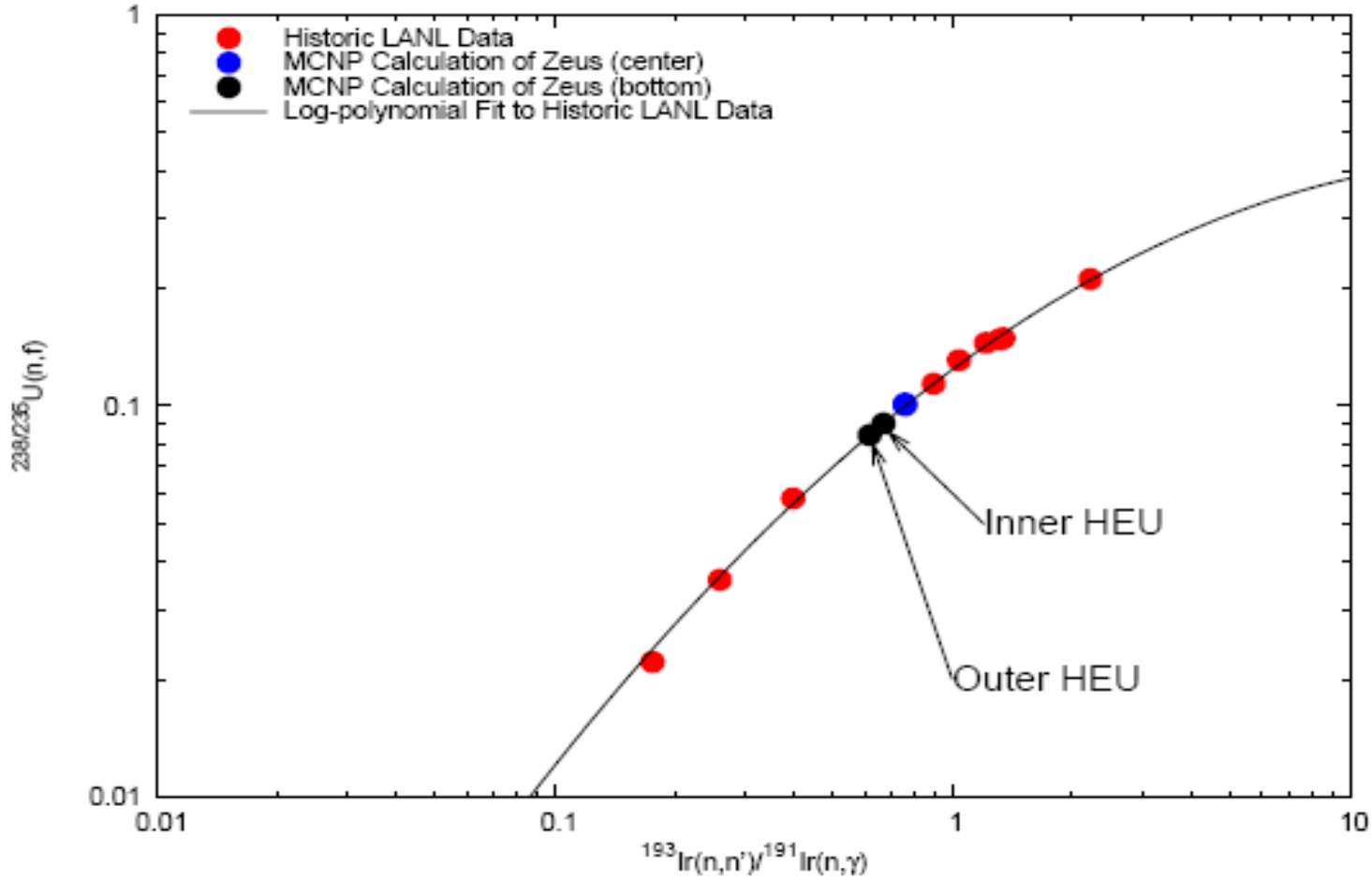

The Zeus Copper/Uranium Critical Experiment

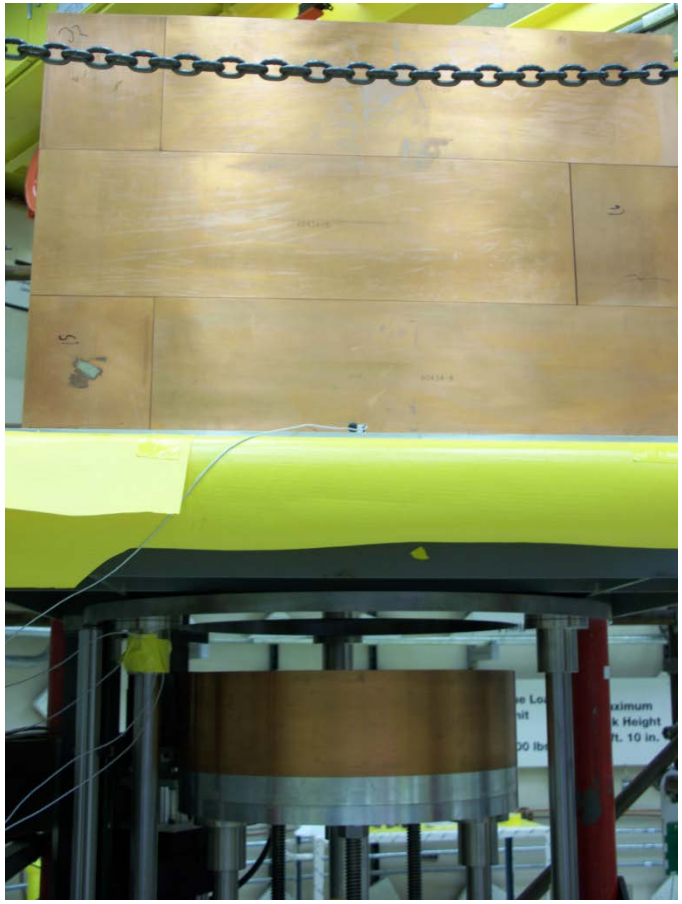

Hand Stacking Operation

Units	Total Counts	M	1/M	Predicted Critical	3/4 Rule	1/2 Rule
1	1904	1	1-	-	-	
2	2109	1.108	0.903	11.309	8.482	6.655
3	2472	1.298	0.770	8.789	6.592	5.895
4	3203	1.682	0.594	7.375	5.531	5.688

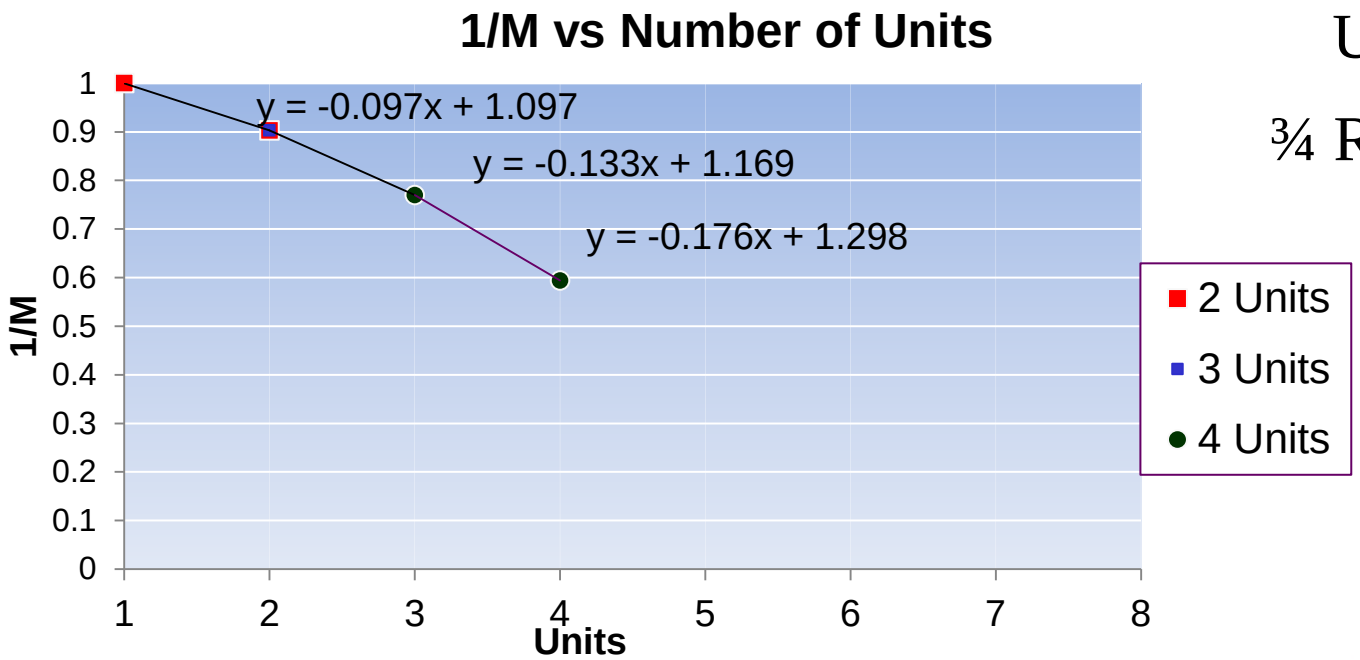

Unit = 12.382 kg

¾ Rule = 68.484 kg

Transferring from bottom to the top

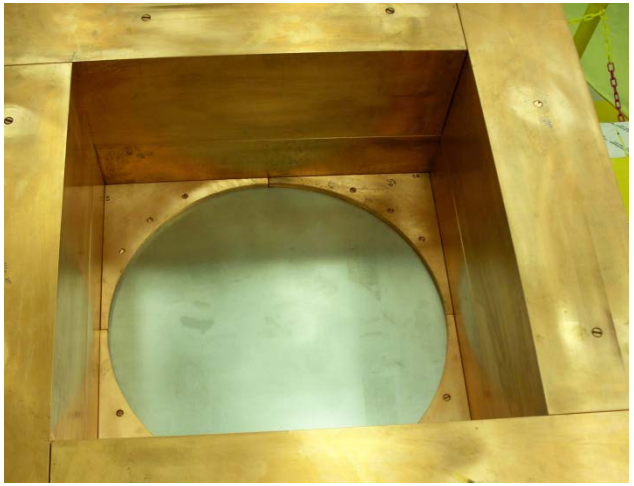

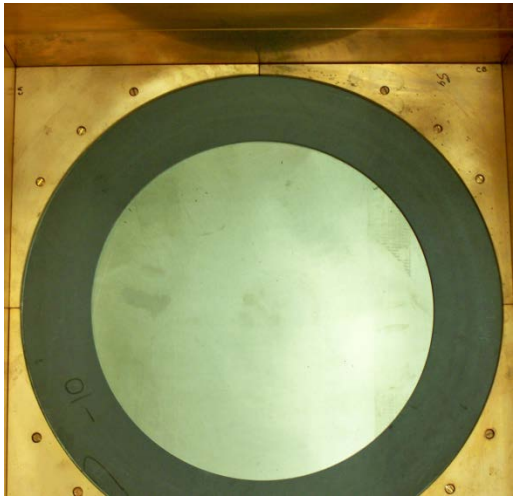

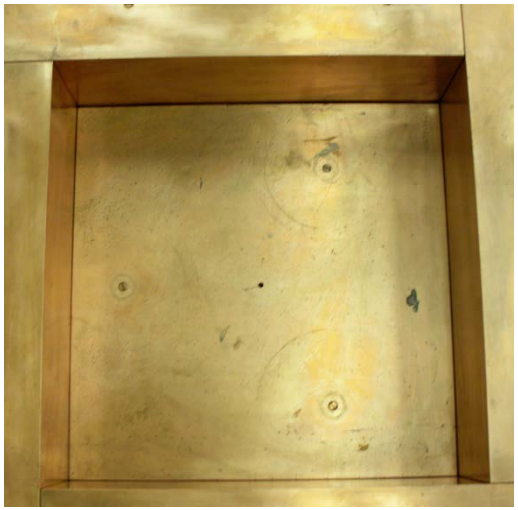

Remote Approach

Mass	1/M	Extrapolation
74998.7	1	
87556.7	0.482792	99116.612
99155.2	0.068566	101075.2086
99924.6	0.00731	100017.5846

1/M vs Uranium Mass

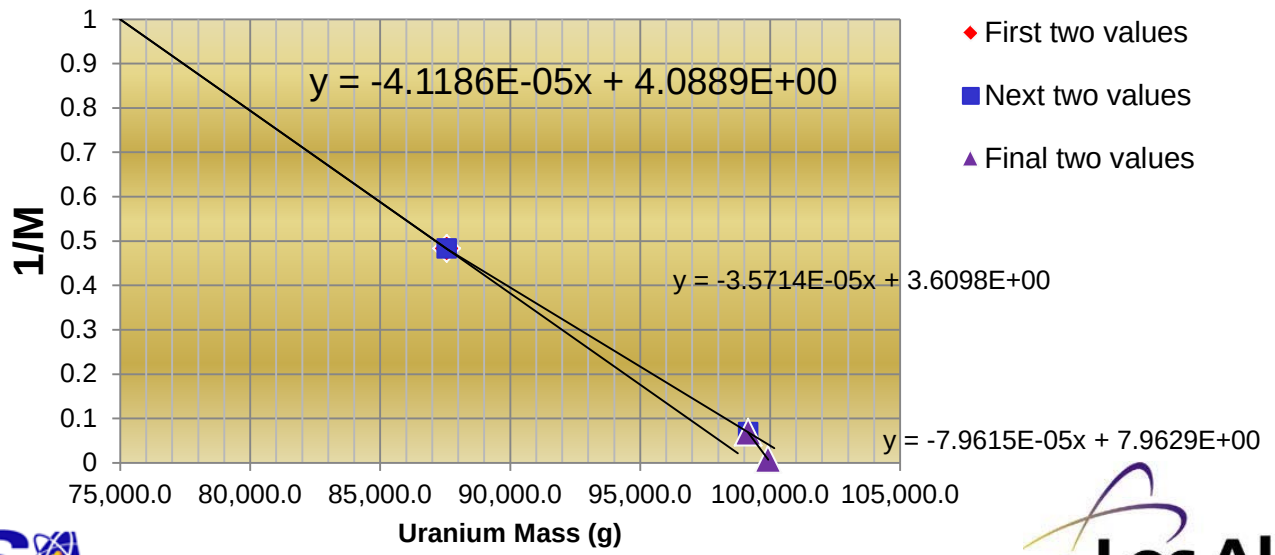

Final Configuration

Upper Portion of the Core					
Part Number	Description	Weight (g)	Part Number	Description	Weight (g)
B-2444-01	Outer Ring 21-in OD 15-in ID	6122.4	10464	Inner Disk 15-in OD 2.5-in ID	6259.2
B-2444-02	Outer Ring 21-in OD 15-in ID	6131.2	10475	Inner Disk 15-in OD 2.5-in ID	6235.8
B-2444-13	Outer Ring 21-in OD 15-in ID	6027.7	11017	Inner Disk 15-in Diameter Solid Plate	6516.8
B-2444-19	Outer Ring 21-in OD 15-in ID	6135.0	11149	Inner Disk 15-in Diameter Solid Plate	6405.4
B-2444-10	Outer Ring 21-in OD 15-in ID	6137.7	11147	Inner Disk 15-in Diameter Solid Plate	6523.6
B-2444-27	Outer Ring 21-in OD 15-in ID	6074.7	11150	Inner Disk 15-in Diameter Solid Plate	6429.2
Bottom Portion of the Core					
B-2444-33	Outer Ring 21-in OD 15-in ID	6158.6	10491	Inner Disk 15-in OD 2.5-in ID	6391.7
B-2444-29	Outer Ring 21-in OD 15-in ID	6131.7	10467	Inner Disk 15-in OD 2.5-in ID	6336.4
Aluminum Plate					
Total Uranium Mass 100,017.1 g					

Cross Section View of the Zeus All Oralloy Experiments

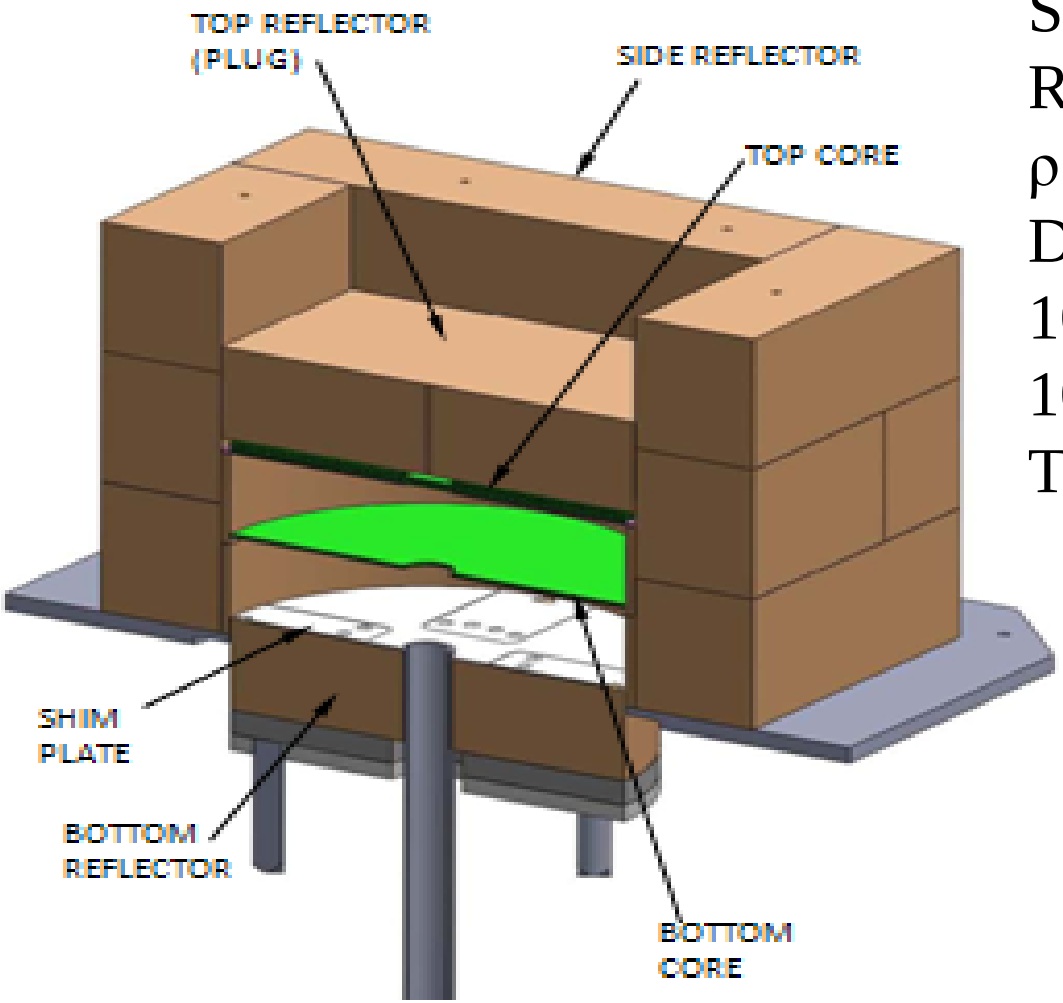

September 8, 2011

Reactor period= 66.97 s

ρ = 12.67 cents

Dose Rate

100 R/hr γ at 10 ft

10000 R/h at foot

Total operation time = 3955 s

Comet Operation

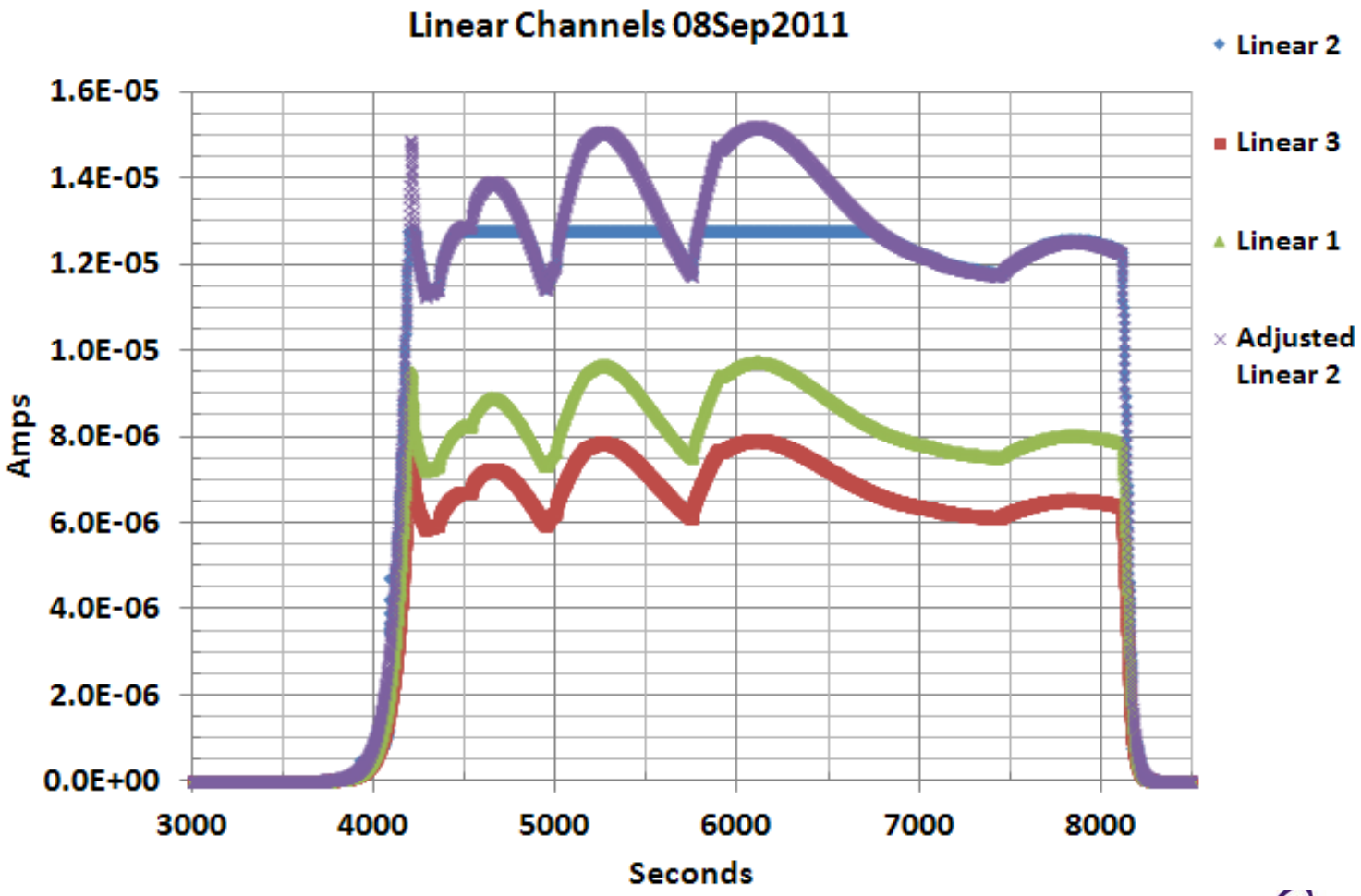

Irradiation of Foils

Target	LANL ID	Target Mass (mg)
U-235	4111	63.8
U-238	4112	580.3
Pu-239	4113	389.9
Ga	4114	60.87
Ir	4115	107.45
Au	4116	127

September 12, 2011
3.75 days after EOB,
the foils were retrieved from the assembly and moved to NCERC counting room for initial gamma spectroscopy.

Most of them arrived at LANL September 20, 2011.

Irradiated Foils at LANL

The HEU and DU foils were dissolved using HNO_3 and HCl.

For the Pu foil, after dissolving the nickel cladding, the Pu disk dissolved using concentrated HNO_3 and HF at 200 ºC.

For the iridium foil, K_2IrCl_6 (potassium hexachloroiridate), was dissolved and chemically separated.

The separated samples were β and γ counted.

The calculate fission per gram of (Pu, Du, and HEU) were estimated based on the ^{99}Mo fission yield activity (5.94% ^{235}U, 5.98% ^{239}Pu, and 6.17% for ^{238}U).

Fission Cross Section

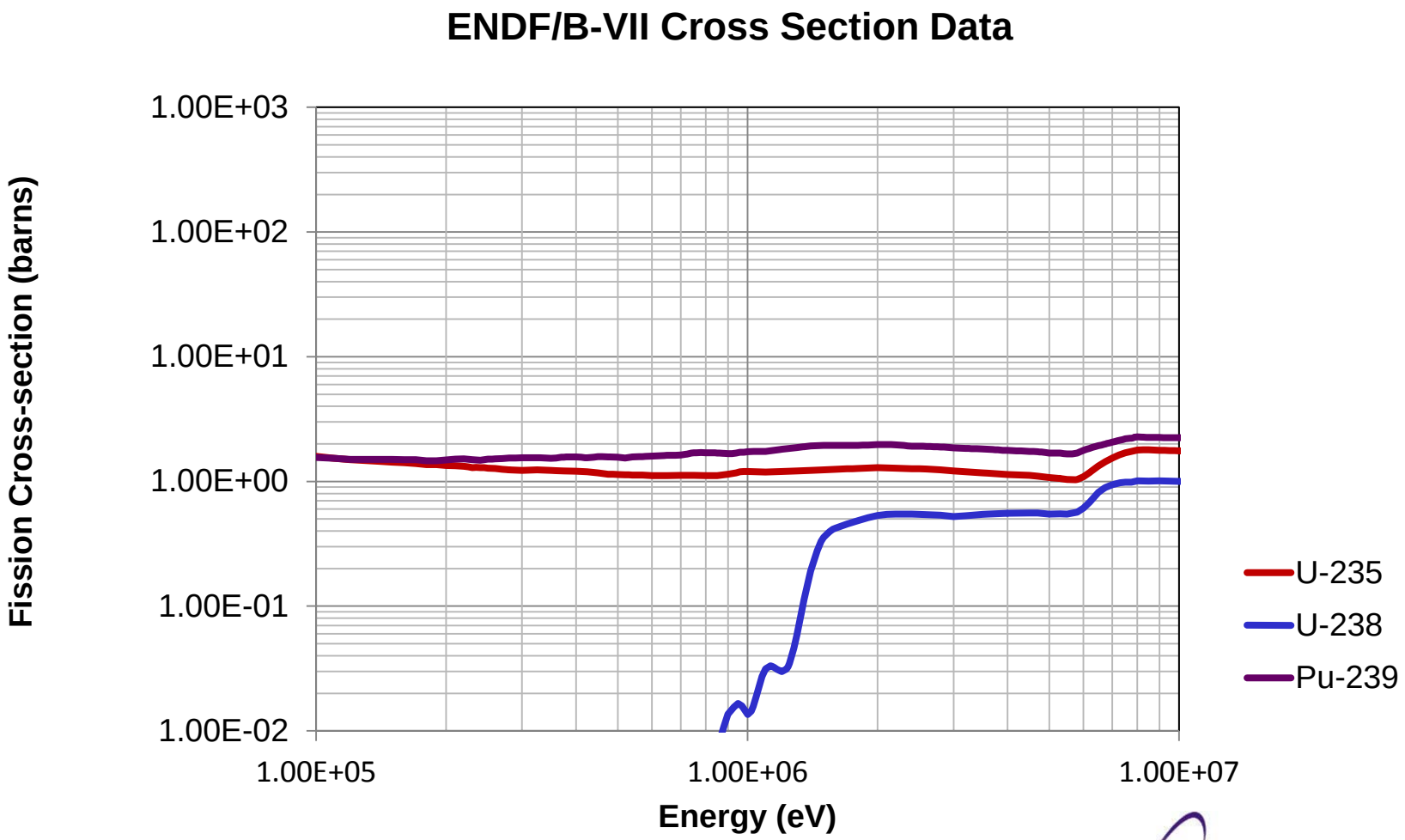

Iridium Absorption Cross Section

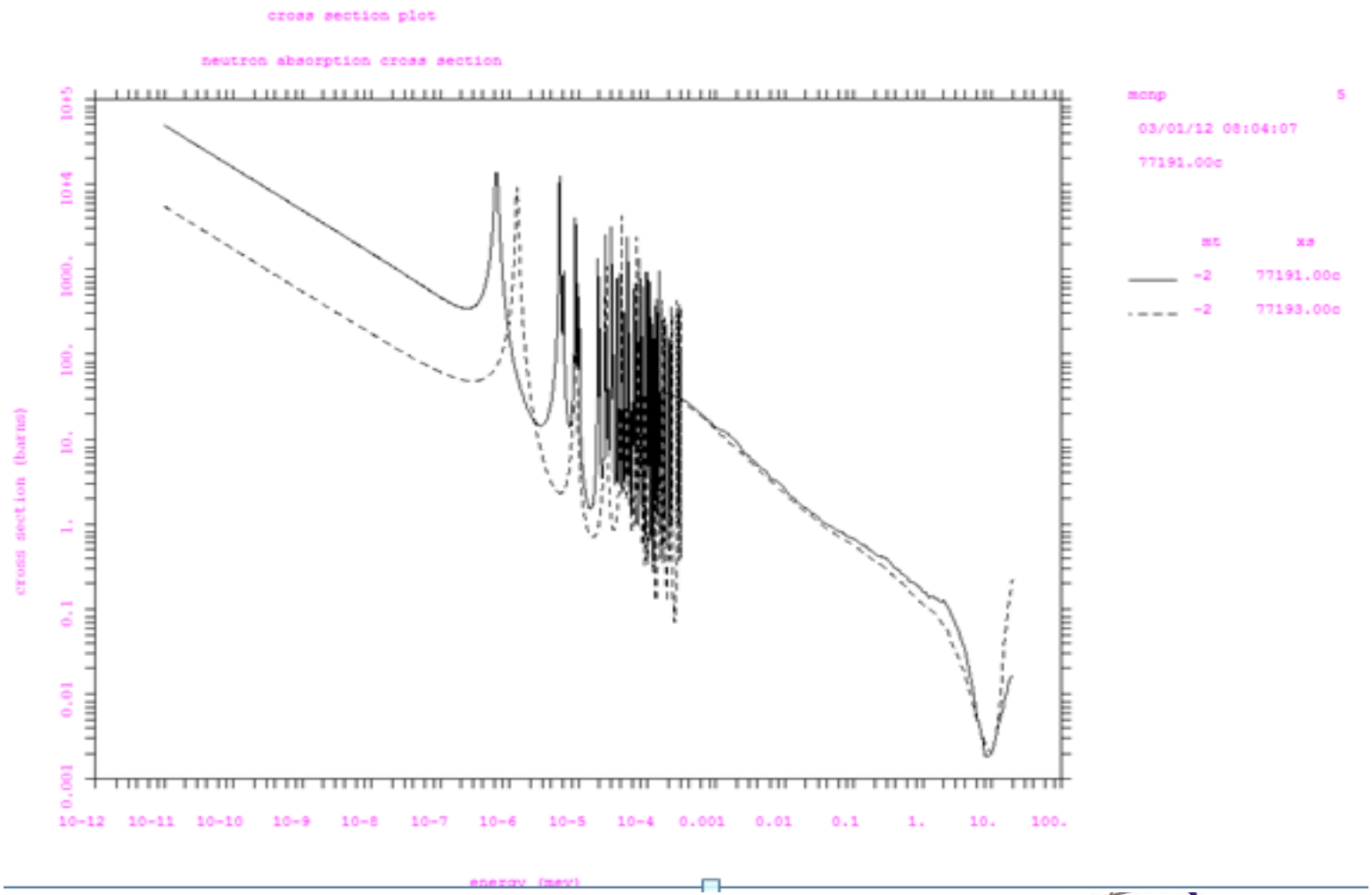

Experimental Results (Pu, DU, HEU, Ir)

Zeus all oralloy critical experiment			
Total number of fissions /gram			
^{235}U	^{238}U	^{239}Pu	
2.84e+12 ± 0.2%	2.56e+11 ± 0.3%	3.89e+12 ± 0.3%	
Critical Assembly	$\frac{\bar{\sigma}_f}{\bar{\sigma}_f}\frac{(U^{235})}{U^{238}}$	$\frac{\bar{\sigma}_f}{\bar{\sigma}_f}\frac{(Pu^{239})}{U^{235}}$	$\frac{\bar{\sigma}_f}{\bar{\sigma}_f}\frac{(Pu^{239})}{U^{238}}$
Zeus all Oy	11.07	1.37	15.18
Godiva Bare Oy-94[3]	6.5	1.42	9.23
Topsy (Oy 94 in thick U)[3]	7.3	1.40	10.22

Isotope	Atoms / g sample @ EOB
Ir-189	7E+06 (limit)
Ir-190	8.7E+08 ± 50.3%
Ir-192	1.215E+11 ± 0.7%
Ir-193m	6.07E+10 ± 1.5%

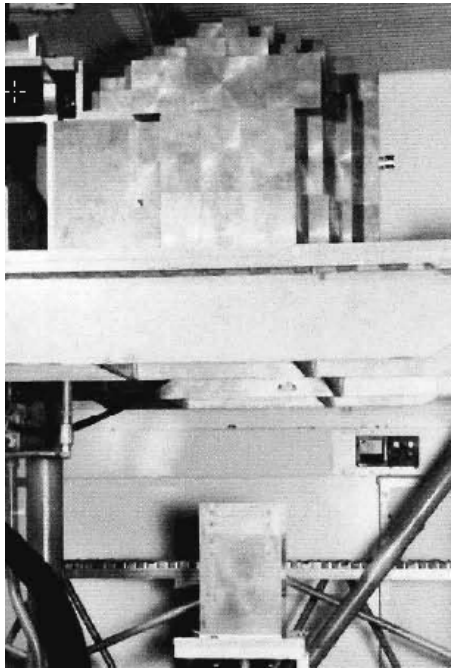

Topsy

Experiment vs Calculation

Reference
C. Wilkerson, Memo to W. Myers
"Zeus/Comet Irradiation," Aug 1, 2011

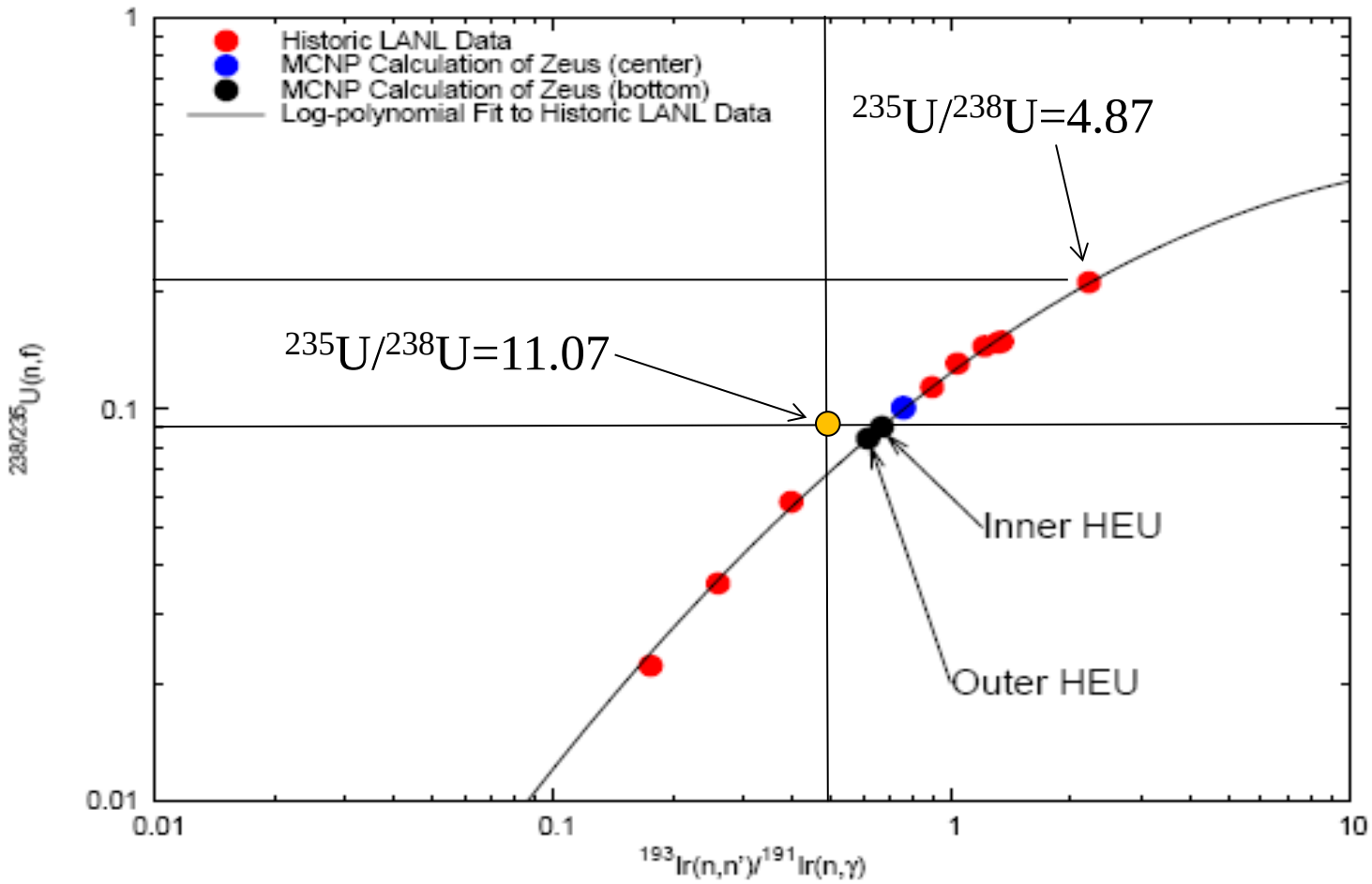

$^{238}U/^{235}U=0.09$

$^{193}Ir/^{191}Ir=0.499$

Primary Neutrons

Reference
Statistical Aspects of Pile Theory
Frederic de Hoffman

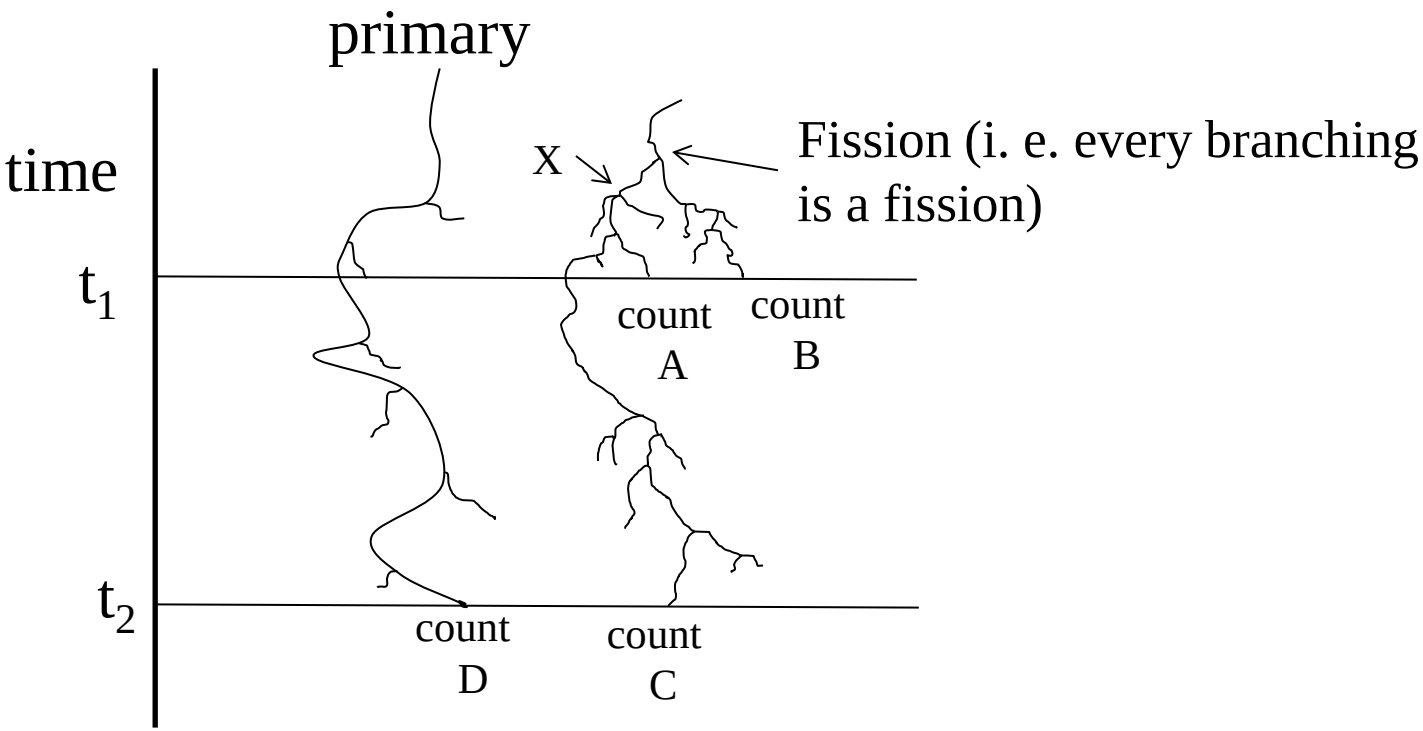

Recording of Neutron Pulses and Analyzing the Data

10,000 time bins

$\rho = -0.10\$$

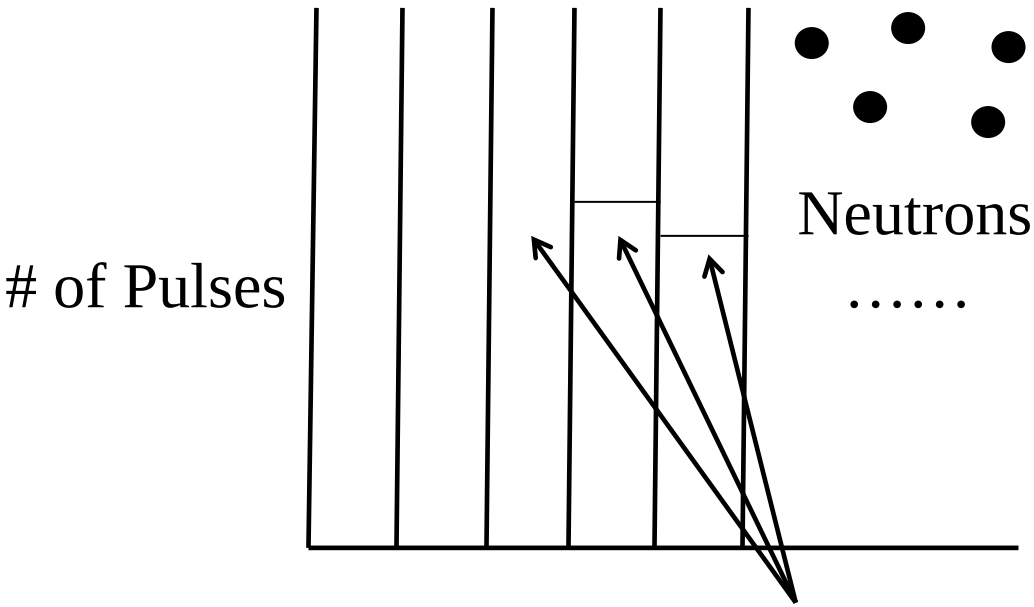

1 μsec time bins

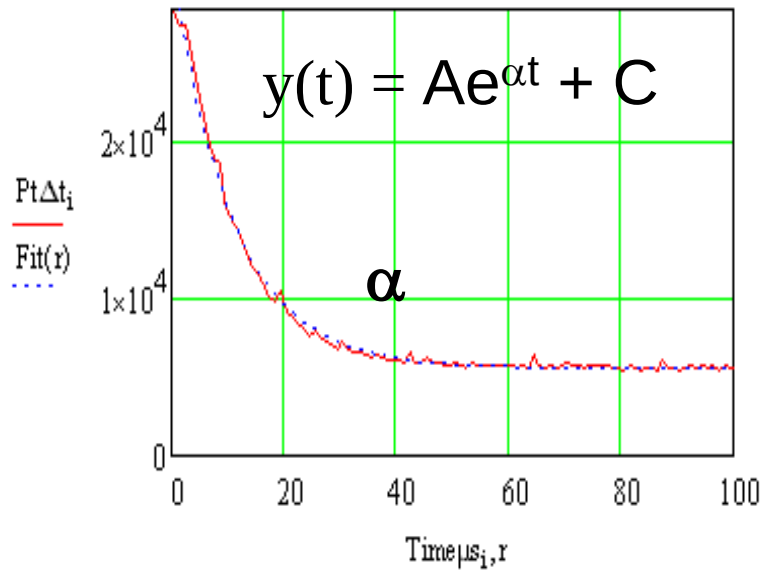

Alpha at Delayed Critical

Alphas vs Inverse Count Rate

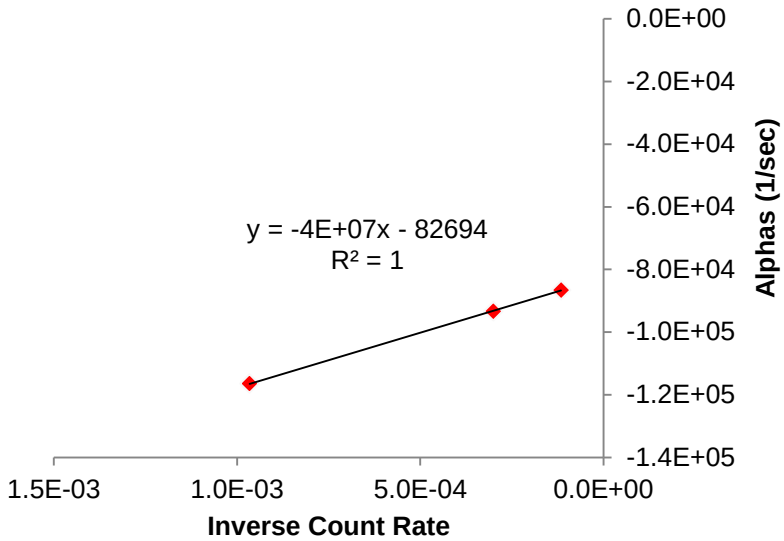

$\alpha(dc) = -82694\ s^{-1} \pm 1.3\%$

$$\alpha = \frac{k_p - 1}{l}$$

$$\alpha_{dc} = \frac{1 - \beta - 1}{l} = \frac{-\beta}{l}$$

β =0 0.0065

$$l = \frac{-\beta}{\alpha(dc)} = 7.86e^{-8}\ \text{sec}$$

National Nuclear Security Administration

Los Alamos NATIONAL LABORATORY

Results and Comparison (Rossi-α)

Assemblies	α (dc)	(neutron lifetime)
Lady Godiva (bare Oy-94)	$-1.1 \times 10^{6}\ s^{-1}$	5.9×10^{-9} s
Godiva IV (bare Oy-93 and 1.5 wt% Mo)	$-8.4 \times 10^{5}\ s^{-1}$	7.7×10^{-9} s
Caliban (bare Oy-90 and 10 wt% Mo)	$-6.5 \times 10^{5}\ s^{-1}$	1.0×10^{-8} s
Topsy (Oy-94 in thick NU)	$-3.7 \times 10^{5}\ s^{-1}$	1.75×10^{-8} s
Big-Ten (10 wt% U)	$-1.2 \times 10^{5}\ s^{-1}$	5.55×10^{-8} s
Zeus (all-oralloy reflected with copper	$-8.3 \times 10^{4}\ s^{-1}$	7.86×10^{-8} s
SHEBA (Solution High Energy Burst Assembly	$-200\ s^{-1}$	4.0×10^{-5} s

Conclusions

- As far as the spectral indices, the indices for this experiment compare quite well with other experiments (Lady Godiva, Topsy).

- Rossi-α at DC for this experiment compares quite well with other measured critical assemblies.

- It appears that there is a discrepancy between the measured and calculated values.

PHYSOR 2014 – The Role of Reactor Physics Toward a Sustainable Future
The Westin Miyako, Kyoto, Japan, September 28 – October 3, 2014, on CD-ROM (2014)

CALIBAN AND GODIVA-IV MEASUREMENTS USING HELIUM-3 DETECTOR SYSTEMS

J. Hutchinson, A. Sood, M. Smith-Nelson, J. Goda, J. Bounds, W. Myers, T. Cutler, B. Richard, B. Rooney
Los Alamos National Laboratory
jesson@lanl.gov

A. Chapelle, P. Casoli, N. Authier
Commissariat `a l'Energie Atomique et aux Energies Alternatives (CEA) Valduc

ABSTRACT

CALIBAN and Godiva-IV are both fast burst reactors with HEU cores. A description and comparison of the two assemblies is presented. Joint LANL and CEA measurements were conducted to measure configurations on the CALIBAN and Godiva assemblies using He-3 detector systems. Measured configurations included many subcritical configurations at various reactivity states as well as configurations at and above delayed critical. The subcritical and delayed critical measurements were analyzed using the Hage-Cifarelli formalism of the Feynman Variance-to-Mean method. This analysis can be used to calculate the multiplication of each configuration, from which the multiplication factor and reactivity are determined. These results are compared to the reactivity states based upon control rod worth curves and MCNP simulations. For each delayed critical configuration an estimate of the delayed neutron fraction is also calculated. Traditionally subcritical neutron noise methods have not been used on systems at, near, or above delayed critical. This work discusses the use and problems encountered of such methods in this regime. Count rate measurements from the positive period configurations were also very accurate but correlated neutron analysis for these configurations was not successful. Very few data sets which can be analyzed using neutron multiplicity analysis exist over such a large range of reactivity values (-$20 to +$0.14).

Key Words: **fast burst reactor, subcritical measurements, critical experiments, neutron noise, Feynman variance-to-mean, MCNP.**

1. INTRODUCTION

In this work measurements conducted on the CALIBAN and Godiva-IV burst assembly machines are analyzed and compared. The CALIBAN reactor is located at the CEA Valduc center in France. Godiva-IV is located at the National Criticality Experiments Research Center (NCERC) at the Nevada National Security Site (NNSS). Joint measurements with LANL and CEA were conducted on both of these assemblies. The CALIBAN measurements were performed in June 2012 and the Godiva-IV measurements were performed in July 2013.

On each assembly, measurements were conducted on many configurations that covered a large range of reactivity values (-$20 to +$0.14). On CALIBAN, 17 configurations were measured: 13 were subcritical, two were at delayed critical, and two were above delayed critical. For Godiva, 18 configurations were measured: 12 were subcritical, 3 were at delayed critical, and 3 were above delayed critical. Multiple configurations at different reactivity states were obtained on both assemblies by varying the safety block (SB) and control rod (CR) positions.

The neutron data that were produced were used to approximate the multiplication of each measured configuration. This can then be used to estimate the multiplication factor and reactivity. These measurements are particularly useful to compare with a known benchmarked system in which one can accurately assess the reactivity and multiplication using a number of methods. Results are also compared with MCNP simulations.

2. DESCRIPTION OF ASSEMBLIES

2.1. Description of the CALIBAN Assembly

The CALIBAN fast burst reactor is made of ten fuel discs and four rods of 93.5 wt.% enriched-uranium metal alloyed with 10 wt.% molybdenum, with a combined weight of 113 kg [1]. The first burst of the CALIBAN reactor occurred in July 1971. Today nearly 2000 super-prompt bursts have been performed on CALIBAN within the authorized excess reactivity of 10 cents above prompt [2]. For this work all of the configurations were below prompt critical so a burst was not performed. The five lower discs that make up the CALIBAN assembly (referred to as “the safety block”) can be raised and lowered remotely. In this work the interface between the 5th disc (top disc of the safety block) and 6th disc (bottom stationary disc) is referred to as the height of the center of the core. Once the safety block is inserted, the three control rods (referred to as “BC1”, “BC2”, and “BC3”) can then be remotely inserted. An excursion rod (referred to as “BE”) is also present but was never inserted for this measurement campaign. Additional information about the CALIBAN reactor can be found in the benchmark evaluation [1].

2.2. Description of the Godiva-IV Assembly

Godiva IV is a fast burst reactor made of approximately 65 kg HEU. Since 1960 nearly 2000 super-prompt bursts have been performed on Godiva [3]. For this work all of the configurations were below prompt critical (a burst was not performed). Godiva consists of 8 fixed HEU components (6 rings plus two smaller cylinders). The safety block, made of approximately 7 kg HEU can be raised and lowered remotely. Once the safety block is inserted, the two control rods (referred to as “CR1” and “CR2”) can then be remotely inserted. Godiva also has a burst rod which was always fully withdrawn for this measurement campaign. Additional information about Godiva IV can be found in the benchmark report [4].

2.3. Similarities and Differences of the Two Assemblies

The design of the CALIBAN assembly originates from the Sandia Pulsed Reactor (SPR) which stemmed from the Godiva fast burst reactors. That being said, it is not surprising that CALIBAN and Godiva-IV have many similarities. Both assemblies contain HEU fuel: 93.16 wt.% ^{235}U for Godiva-IV [4] and 93.417 wt/% ^{235}U for CALIBAN [1]. Both consist of a uranium-molybdenum alloy, but the amount of Mo is quite different: 1.5 wt.% for Godiva-IV [4] and 9.86 wt.% Mo for CALIBAN [1].

The HEU masses of the two assemblies are quite different: 64.4 kg for Godiva-IV versus 113 kg for CALIBAN. This is because the geometries of the cores are quite different as shown in Figure 1. When assembled, the CALIBAN core has an ID 3 cm, an OD of 19.5 cm, and a height of 25.2 cm. Godiva-IV has an OD of 17.78 cm and a height of 15.59 cm. Godiva-IV does not have a constant ID but on average it is less than the ID of CALIBAN.

The three rods for Godiva-IV (two control rods and one burst rod) each have an OD of 2.18 cm and a height of 12.7 cm. The four rods for CALIBAN (three control rods and one burst rod) each have an OD of 2.269 cm and a height of 31.695 cm. The reactivity worth for each of the two Godiva control rods is approximately \$1.20 [3] versus \$2.26 for the three CALIBAN control rods [5]. When the safety block is inserted in Godiva but the control rods are fully withdrawn, the system is approximately \$2.07 below delayed critical (k_{eff} = 0.987). For CALIBAN, this configuration has a reactivity of approximately \$3.72 below delayed critical (k_{eff} = 0.976).

Except where predicted from measurements, this work uses a delayed neutron fraction (β_{eff}) of 659 pcm for both assemblies [6]. It is known that a single delayed neutron fraction for all configurations and reactivities should be avoided but a comprehensive set of measured values for this parameter does not currently exist for either reactor. Having a single value also makes it much easier to compare results from the two assemblies.

Figure 1. CALIBAN core on the left and Godiva-IV core on the right. Both are in their shutdown states (S1 for both assemblies, described in Section 3).

3. DESCRIPTION OF MEASUREMENTS

Three detector systems were present for both measurement campaigns. One is a CEA detector system consisting of 3 He-3 tubes inside polyethylene which has been described in previous work [7]. The second detector present was the LANL Shielded Neutron Assay Probe (SNAP) detector. The SNAP detector contains a single He-3 tube that gives count rate information. The third detector system is the Neutron Multiplication Pod (NPOD) detectors which contain 15 He-3 tubes inside polyethylene and produce list mode (time-tagged) data that can be used for correlated neutron analysis. These data can be analyzed using several different methods. The particular analysis method that was used for this work was the Hage-Cifarelli formulism of the Feynman Variance-to-Mean method. Information on this analysis technique can be found in previous reports [8-9]. More information on the SNAP and NPOD detectors can be found in previous reports [10-11]. This presentation will focus only on the results from the SNAP and NPOD detector systems. Results from the CEA detector system are the focus of several works including a PHD thesis which analyzes data from these measurements [7,12-14].

3.1. Description of the CALIBAN Measurements

In total, 17 configurations were measured: 13 were subcritical, two were at delayed critical, and two were above delayed critical. Multiple configurations at different reactivity states were obtained by varying the safety block and control rod positions. Two different detector positions were used. In position 1, the CEA detector system was located 150 cm radially and 0 cm vertically from the center of the core. The two NPOD detectors were located at a distance of 116.9 cm radially and -58 cm vertically from the center of the core. For position 2, the NPOD and CEA detector systems essentially switched positions. The CEA detector system was located 116.9 cm radially and -58 cm vertically from the center of the core. Only one NPOD detector was used in position 2 and was located 150 cm radially and 0 cm vertically from the center of the core. This work will focus on the results from position 2 as nearly every configuration was measured at this position. In both position 1 and 2 the SNAP detector was located at a distance of 174.1 cm radially and 0 cm vertically from the center of the core. Results from the SNAP and NPOD detectors are also available in previous works [15-17].

For the subcritical measurements a Cf-252 source was placed in the glory hole of the CALIBAN core. This source had a strength of 1.14e6 n/s when the measurements took place. The entire CALIBAN core and driving units are placed on a lift so that the entire core can be lowered into a pit. This allowed for “background” measurements to be performed with and without the Cf-252 source present with CALIBAN in the pit. The Cf-252 source was not present for the positive period measurements.

Table 1 shows the element positions that were used for each of the 17 configurations in order of increasing reactivity. These element positions were recorded from the CALIBAN control system. As shown in the table, 13 of the configurations were subcritical (referred to as S1 through S13). As can be seen, the first 8 configurations are referred to by the safety block positions (and all of the control rods are fully withdrawn). In configuration S8 the safety block is fully inserted (70.532 mm of insertion). For the configurations listed after S8, the safety block is fully inserted and the control rods were inserted to the positions listed. Configurations S9 through S13 are referred to by their expected reactivity values. In order to achieve these configurations, the distance of a single (or combination) of control rods that equals the desired subcritical reactivity was inserted. The other control rods were then inserted to achieve a delayed critical configuration. After it was confirmed that the system was at delayed critical the control rod(s) with a total worth equal to the desired subcritical reactivity were fully withdrawn. As can be seen in Table 1 there were two delayed configurations that were measured (referred to as DC1 and DC2). Both configurations were at the same reactivity level but were achieved using control rod elements at different positions. The last two configurations were on a positive period (above delayed critical). They are referred to as PP1, which had a 500 second period and PP2 which had a period of 60 seconds.

Table 1. Element positions for CALIBAN configurations.

		Element Positions (in mm)			
Configuration		SB position	BC1	BC2	BC3
SB out	S1	0.089	0.000	0.000	0.000
SB 10mm	S2	9.970	0.000	0.000	0.000
SB 20mm	S3	20.019	0.000	0.000	0.000
SB 40mm	S4	40.019	0.000	0.000	0.000
SB 60mm	S5	60.009	0.000	0.000	0.000
SB 65mm	S6	65.032	0.000	0.000	0.000
SB 67.5mm	S7	67.501	0.000	0.000	0.000
SB in	S8	70.531	0.000	0.000	0.000
300 cent subcritical	S9	70.529	5.550	90.850	6.080
200 cent subcritical	S10	70.530	120.000	82.630	5.710
150 cent subcritical	S11	70.531	120.000	118.510	6.100
100 cent subcritical	S12	70.531	205.120	69.900	7.000
80 cent subcritical	S13	70.531	205.100	87.700	6.790
delayed critical	DC1	70.532	205.120	69.970	110.000
delayed critical	DC2	70.531	205.100	87.700	96.200
500 second period	PP1	70.532	205.100	50.000	127.590
60 second period	PP2	70.532	205.100	50.000	135.590

3.2. Description of the Godiva-IV Measurements

Table 2 shows the element positions that were used for each of the 18 configurations in order of increasing reactivity. These element positions were recorded from the Godiva control system. A value of 0 indicates that the element is fully inserted (note this is the opposite of CALIBAN where 0 was fully withdrawn). As shown in the table, 12 of the configurations were subcritical (referred to as S1 through S12). Similar to CALIBAN, the first 7 configurations are referred to by the safety block position (all of the control rods are fully withdrawn for these configurations). For the configurations listed after S7, the safety block is fully inserted and the control rods were inserted to the positions listed in the table. Configurations S8 through S12 are referred to by their expected reactivity values. In order to achieve these configurations a delayed critical state was first achieved. The control rod(s) would then be removed based on control rod worth curves so that the desired reactivity was achieved. As can be seen in Table 2 there were 3 delayed critical configurations that were measured (referred to as DC1 through DC3). The last three configurations were on a positive period (above delayed critical). They are referred to as PP1 through PP3.

For the Godiva-IV measurements, the CEA detector system was located 200 cm radially and 0 cm vertically from the center of the core. The NPOD detector was 100 cm radially and 3 cm vertically from the center of the core. The SNAP detector was located at a distance of 100 cm radially and 0 cm vertically from the center of the core.

Table 2. Element positions for Godiva-IV configurations.

		Element Positions (in inches)		
Configuration		SB position	CR1	CR2
SB out	S1	7.844	4.050	4.050
SB 2.083"	S2	2.083	4.050	4.050
SB 0.994"	S3	0.994	4.050	4.050
SB 0.544"	S4	0.544	4.050	4.050
SB 0.272"	S5	0.272	4.050	4.050
SB 0.161"	S6	0.161	4.050	4.050
SB in	S7	-0.130	4.050	4.050
200 cents subcritical	S8	-0.130	3.606	3.504
150 cents subcritical	S9	-0.130	2.258	2.448
100 cents subcritical	S10	-0.130	1.706	1.655
75 cents subcritical	S11	-0.130	1.344	1.304
50 cents subcritical	S12	-0.130	1.048	1.000
Delayed critical	DC1	-0.130	0.312	0.311
Delayed critical	DC2	-0.130	0.363	0.364
Delayed critical	DC3	-0.130	0.158	0.151
500 sec period	PP1	-0.130	0.097	0.151
180 sec period	PP2	-0.130	0.097	0.057
120 sec period	PP3	-0.130	0.023	0.057

For most of the measurements, a Cf-252 source was placed in the glory hole of Godiva. This source had a strength of 2.24e5 n/s when the measurements took place. The Cf-252 source was present for all of the subcritical configurations and two of the delayed critical configurations (DC1 and DC2). The source was not present for DC3 and the positive period measurements.

It should be noted that configurations with the same names for the Godiva-IV and CALIBAN do not have the same multiplication or reactivity. The only configurations that should be directly compared are the -$2.00 (S8 on Godiva vs S10 on CALIBAN), -$1.50 (S9 on Godiva vs S11 on CALIBAN), -$1.00 (S10 on Godiva vs S12 on CALIBAN), delayed critical, and 500 sec period (PP1 for both Godiva and CALIBAN) configurations.

4. RESULTS

4.1. Subcritical Results

The SNAP detector count rates are shown for each of the subcritical configurations in Figure 2. It should be noted that the values on the x-axis refer to the subcritical configuration numbers (a value of 1 was configuration S1). That being said, the configuration numbers increase as the reactivity increases but not at any set rate (the reactivity increase between S1 and S2 is different than between S2 and S3). That being said, one should not expect to see any shape for the results curves (other than an increase in count rates and multiplication). The CALIBAN and Godiva data in Figure 2 cannot be directly compared since the Cf-252 source strength and detector placement were different. The count rates for the two positions on CALIBAN were nearly identical (this is not surprising since the SNAP location remained stationary).

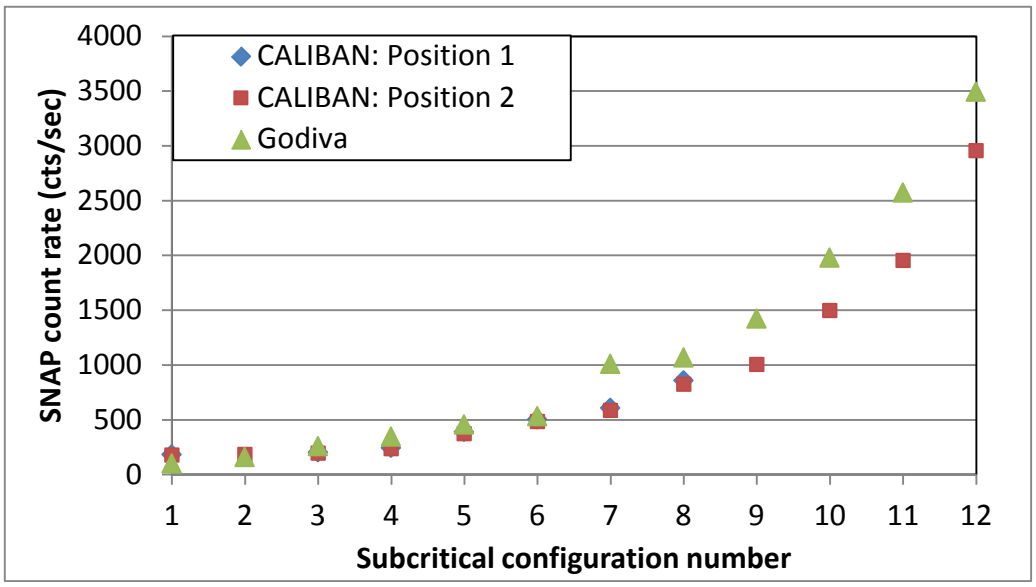

Figure 2. SNAP count rate for the CALIBAN and Godiva subcritical configurations.

The NPOD singles and doubles counting rates (values derived from the first and second reduced factorial moments in the Hage-Cifarelli formulism) are shown in Figure 3. The singles counting rate is simply the count rate of the NPOD detector system. The doubles count rate is essentially the rate of detection of two neutrons from a single fission chain. As one might expect, the configurations at high multiplications resulted in very high count rates. It should be noted that dead time issues are present in some of these measurements which have not been accounted for at this time. Similar to the SNAP data, the CALIBAN and Godiva count rates cannot be directly compared due to detector placement and Cf-252 emission rates.

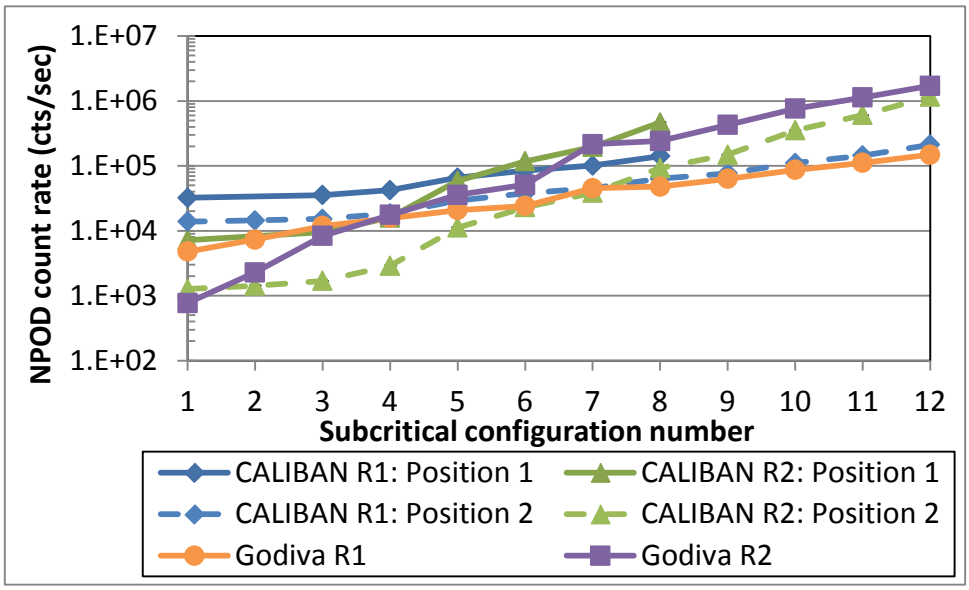

Figure 3. NPOD singles (R1) and doubles (R2) counting rates.

The measured total and leakage multiplication values are shown for each of the configurations in Figure 4. Total multiplication is defined as the average number of neutrons generated from a single starter neutron. Leakage multiplication is the average number of neutrons that escape the system per starter neutron. These were analyzed using the same system of equations with the same nuclear data parameters.

Table 3 shows results for the highly subcritical configurations in which all of the control rods were withdrawn. It can be seen that the measured results compare better with MCNP KCODE calculations as reactivity increases.

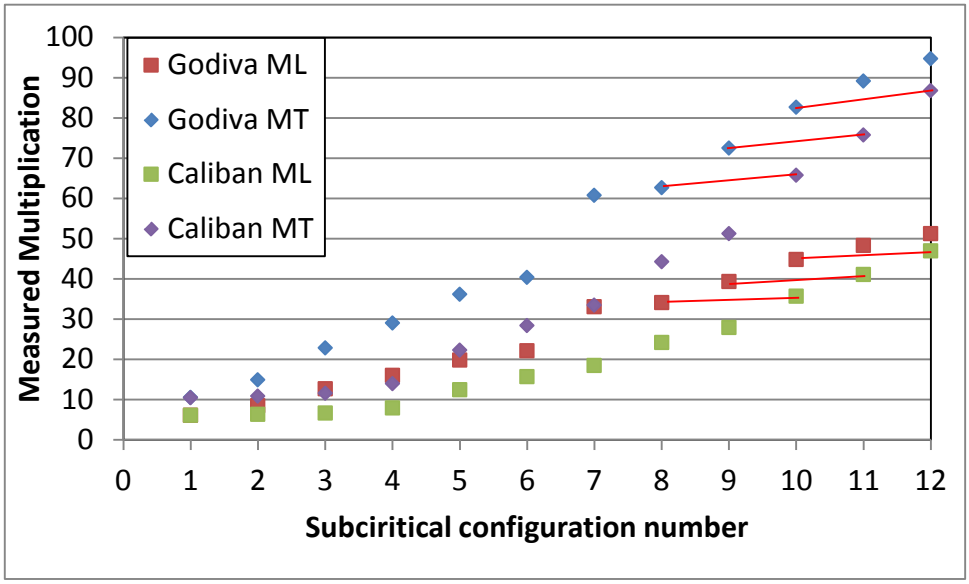

Figure 4. Total (M_T) and leakage (M_L) multiplication calculated from the NPOD measured data. Red lines are drawn between the CALIBAN and Godiva configurations that can be directly compared (those that are at equivalent reactivity states based upon control rod worth curves).

Table 3. Results of configurations in which all control rods are withdrawn.

Assembly	SB Position	Configuration	M_T	keff	MCNP KCODE	C/E
Caliban	SB out	S1	10.5	0.910	0.881	0.968
	SB 10mm	S2	10.9	0.914		
	SB 20mm	S3	11.6	0.920	0.891	0.969
	SB 40mm	S4	13.9	0.934	0.909	0.973
	SB 60mm	S5	22.2	0.961	0.945	0.982
	SB 65mm	S6	28.3	0.971	0.958	0.986
	SB 67.5mm	S7	33.5	0.977	0.965	0.988
Godiva	SB out	S1	10.5	0.911	0.871	0.957
	SB 2.083"	S2	14.9	0.939	0.909	0.968
	SB 0.994"	S3	22.8	0.963	0.943	0.980
	SB 0.544"	S4	29.0	0.972	0.959	0.987
	SB 0.272"	S5	36.1	0.979	0.969	0.991
	SB 0.161"	S6	40.3	0.982	0.974	0.992

As previously mentioned, several configurations (S8-S12 on CALIBAN and S7-S12 on Godiva) were achieved by obtaining a delayed critical state and then removing an element(s) in which the worth of the element was equal to the desired subcritical reactivity. Tables 4-5 show the reactivity values (ρ/β) for these configurations from the control rod worth curves. Given the reactivity, one can easily calculate the effective neutron multiplication factor using $k_{eff} = 1/(1-\rho)$, prompt multiplication factor using $k_p = k_{eff}(1-\beta_{eff})$, and the prompt total multiplication from $M_T = 1/(1-k_p)$. All of these parameters are shown in Tables 4-6. It should be noted that the measured total multiplication includes prompt neutrons only (since delayed neutrons are not correlated in time) which is why it is calculated using k_p.

Also shown in Tables 4-6 are the measured results from the NPOD detectors. Here the total multiplication is calculated first from the data and the multiplication factor is calculated using the same basic equations mentioned above. It can be seen in Tables 4-6 that the C/E for k agrees very well with the control rod worth curves (C is from the control rod worth curves and E is from the measured data). The C/E for multiplication should only be used up to a certain point since this parameter is approaching infinity as the system approaches criticality. For CALIBAN, the largest difference in k_{eff} values between the control rod worth curves and the measured data was 0.008 for configuration S8 and the best agreement was $\Delta k_{eff} = 0.002$ for configuration S12. For Godiva, Δk_{eff} values of 0.004 (for configuration S8) and 0.0003 (for configuration S11) gave the worst and best agreements respectively.

Tables 4-6 also have results from KCODE calculations using MCNP. The k_{eff} values presented in these tables were not calculated directly. The CALIBAN benchmark model yielded a k_{eff} of 1.00816 +/- 0.00017 [18]. A bias of 0.00816 was subtracted from all of the MCNP KCODE calculations for each configuration. For Godiva, the simulations of the three delayed critical configurations yielded an average k_{eff} of 0.98991 (each had a standard deviation of 0.00018). This value is close to 0.98983, which is the average of Cases 1-4 in the benchmark evaluation [4]. For Godiva, a bias of 0.01009 (calculated by subtracting 0.98991 from 1) was added to the MCNP criticality eigenvalue for each configuration. It can be seen in Tables 4-6 that the bias-adjusted simulation results agree well with the control rod worth curves. It can also be seen the measured and simulated results agree very well. For CALIBAN, the largest difference in k_{eff} values between the measured data and simulations was 0.009 for configuration S8 and the best agreement was $\Delta k_{eff} = 0.002$ for configuration S12. For Godiva, Δk_{eff} values of 0.004 (for configuration S8) and 0.0003 (for configuration S12) gave the worst and best agreements respectively.

Table 6 has the same data as Tables 4 and 5 but focuses on the three subcritical configurations that can be directly compared for the two assemblies (-$2.00, -$1.50, and -$1.00). It can be seen in this table that the results from Godiva and CALIBAN are nearly identical. It can be seen in Table 6 and Figure 4 that the data from CALIBAN predicted slightly higher multiplication values for all three configurations. The Δk_{eff} values found by subtracting the Godiva measurements from the CALIBAN measurements were 0.0007 for -$2.00 and 0.0006 for both -$1.50 and -$1.00.

Table 4. Results from CALIBAN subcritical configurations.

	Configuration	S8	S9	S10	S11	S12
Control rod worth curves	ρ/β ($)	-3.72	-3.00	-2.00	-1.50	-1.00
	ρ	-0.025	-0.020	-0.013	-0.010	-0.007
	k_{eff}	0.976	0.981	0.987	0.990	0.993
	k_p	0.970	0.974	0.980	0.984	0.987
	M_T	32.9	38.7	51.2	61.3	76.4
NPOD Feynman Analysis	M_T	44.2	51.2	65.7	75.7	86.7
	k_p	0.977	0.980	0.985	0.987	0.988
	k_{eff}	0.984	0.987	0.991	0.993	0.995
	C/E M_T	0.745	0.756	0.780	0.809	0.881
	C/E k	0.992	0.994	0.996	0.997	0.998
MCNP KCODE (bias adjusted)	k_{eff}	0.975	0.981	0.988	0.991	0.993
	k_p	0.969	0.974	0.981	0.984	0.986
	M_T	31.8	39.1	53.0	63.0	73.5
	C/E M_T	1.037	0.991	0.967	0.973	1.039
	C/E k	1.001	1.000	0.999	1.000	1.001

Table 5. Results from Godiva subcritical configurations.

	Configuration	S7	S8	S9	S10	S11	S12
Control rod worth curves	ρ/β ($)	-2.07	-2.00	-1.50	-1.00	-0.75	-0.50
	ρ	-0.014	-0.013	-0.010	-0.007	-0.005	-0.003
	k_{eff}	0.987	0.987	0.990	0.993	0.995	0.997
	k_p	0.980	0.980	0.984	0.987	0.989	0.990
	M_T	50.0	51.2	61.3	76.4	87.1	101.5
NPOD Feynman Analysis	M_T	60.7	62.6	72.5	82.7	89.1	94.7
	k_p	0.984	0.984	0.986	0.988	0.989	0.989
	k_{eff}	0.990	0.991	0.993	0.994	0.995	0.996
	C/E M_T	0.824	0.818	0.846	0.924	0.978	1.072
	C/E k	0.996	0.996	0.997	0.999	1.000	1.001
MCNP KCODE (bias adjusted)	k_{eff}	0.986	0.987	0.990	0.993	0.995	0.996
	k_p	0.979	0.980	0.984	0.986	0.988	0.990
	M_T	48.0	50.3	60.7	73.2	85.5	97.0
	C/E M_T	1.042	1.019	1.010	1.043	1.019	1.046
	C/E k	1.001	1.000	1.000	1.001	1.000	1.000

Table 6. Comparison of CALIBAN and Godiva results at -$2.00, -$1.50, and -$1.00.

	Assembly	Godiva	CALIBAN	Godiva	CALIBAN	Godiva	CALIBAN
Control rod worth curves	ρ/β ($)	-2.00		-1.50		-1.00	
	ρ	-0.013		-0.010		-0.007	
	k_{eff}	0.987		0.990		0.993	
	k_p	0.980		0.984		0.987	
	M_T	51.2		61.3		76.4	
NPOD Feynman Analysis	M_T	62.6	65.7	72.5	75.7	82.7	86.7
	k_p	0.984	0.985	0.986	0.987	0.988	0.988
	k_{eff}	0.991	0.991	0.993	0.993	0.994	0.995
	C/E M_T	0.818	0.780	0.846	0.809	0.924	0.881
	C/E k	0.996	0.996	0.997	0.997	0.999	0.998

4.2. Delayed Critical Results

To achieve a delayed critical configuration, a state above delayed critical was first established and the desired power level was obtained. The rods were then adjusted to achieve a delayed critical configuration. For the configurations with a Cf-252 source, the lowest power level possible was desired. In Table 7 the definition of delayed critical (k_{eff} = 1 and ρ = 0) is compared with the measured NPOD data and MCNP simulations. The NPOD results were analyzed using the Hage-Cifarelli formulism of the Feynman Variance-to-Mean method just like the subcritical configurations.

Correlated neutron methods have not been traditionally used for configurations at and above delayed critical. One should ask, therefore, if these methods can even be accurate in this regime. All prompt neutrons are produced in a very small time period after the fission event in which they were created occurs (around 10^{-14} sec). This is why all prompt neutrons are correlated in time. Delayed neutrons, however, occur much later in time (the fastest delayed neutron group has a half-life on the order of a tenth of second). Nearly all subcritical measurement methods look at data grouped into time bins. The width of the bin can vary but is generally between 100 nsec to 10 msec (1 μsec to 5 msec bins are commonly used). Therefore any estimated multiplication values include only prompt neutrons. This is why the total multiplication was defined as $M_T=1/(1-k_p)$. Between delayed and prompt critical all systems are subcritical on prompt neutrons alone so correlated neutron measurement methods should work in this regime.

It can be seen that the measured data compared very well (all within 150 pcm of the delayed critical definition). In addition, the measured and simulated results were also very similar (all within 200 pcm). Both the Valduc and LANL facilities have detectors which use count rates to estimate the reactor period (which was then used to calculate a reactivity using the Inhour equation). Instead of using correlated neutron analysis, the total count rate of the NPOD can be used in the same way. Both the NPODs and facility detector systems calculated that all four delayed critical configurations were within 1 cent of delayed critical.

Since it is known that both configurations were at delayed critical, one can use the measured k_p

value to estimate β_{eff}. This resulted in β_{eff} values as shown in Table 8. All of the values are within 20% of the assumed value of 659 pcm. It should be noted that correlated neutron measurements are likely not the most accurate method to estimate β_{eff}.

Table 7. Results from the delayed critical configurations.

	Assembly	CALIBAN	Godiva	CALIBAN	Godiva
	Configuration	DC1	DC2	DC2	DC3
	Position	2	-	1	-
	Cf source	Yes	Yes	No	No
Delayed critical definition	ρ/β ($)	0			
	ρ	0			
	k_{eff}	1.000			
	k_p	0.993			
	M_T	151.7			
NPOD Feynman Analysis	M_T	170.9	182.4	177.1	127.7
	k_p	0.994	0.995	0.994	0.992
	k_{eff}	1.001	1.001	1.001	0.999
	ρ	7.43E-04	1.11E-03	9.49E-04	-1.25E-03
	ρ/β ($)	0.11	0.17	0.14	-0.19
	C/E M_T	0.888	0.832	0.857	1.189
	C/E k	0.999	0.999	0.999	1.001
MCNP KCODE (bias adjusted)	k_{eff}	0.999	1.000	1.000	1.001
	k_p	0.992	0.993	0.993	0.994
	M_T	131.7	144.3	152.2	165.5
	C/E M_T	1.152	1.051	0.997	0.917
	C/E k	1.001	1.000	1.000	0.999

Table 8. β_{eff} values from the NPOD measured results for the delayed critical configurations.

Source	Caliban	Godiva	Assumed
Yes	585	548	659
No	565	783	

4.3. Positive Period Results

Positive period configurations were obtained by establishing delayed critical and then inserting the extra reactivity desired using control rod worth curves. Table 9 shows the results of the CALIBAN positive period configurations. Here the desired configuration (from the control rod worth curves) is compared to the Valduc facility detectors and the NPOD detectors. For this table, both the facility and NPOD detectors look only at the count rate to determine the reactor

period. The reactivity is then calculated from the reactor period using the Inhour equation.

Section 4.2 mentioned that correlated neutron analysis should be possible for positive period measurements below prompt critical. The fact that the count rate is changing above delayed critical, however, creates an issue that must be taken into account. At this time, both LANL and CEA have attempted to use correlated neutron measurements from these data and have failed to produce consistent results. This could be due to the changing count rate, overlapping fission chains, dead time, or a combination of these. For this reason, correlated neutron data is not presented for the configurations above delayed critical. This is an area of interest for future research.

Results of the Godiva positive period configurations are shown in Table 10. Here the count rate in the NPOD detector is compared to the desired configuration (control rod worth curves) and two sets of facility detectors: the startups are He-3 tubes in pulse mode and the linears are compensated ion chambers in current mode.

Table 9. Results from the CALIBAN positive period configurations.

	Configuration	PP1	PP2
Desired configuration	Reactor Period (sec)	500	60
	ρ/β ($)	0.02	0.14
	k_{eff}	1.000	1.001
	k_p	0.994	0.994
	M_T	155.5	177.1
Valduc detectors	Reactor Period (sec)	508	61
	ρ/β ($)	0.02	0.14
	k_{eff}	1.000	1.001
	k_p	0.994	0.994
	M_T	155.4	176.8
NPOD count rate	Reactor Period (sec)	526	68
	ρ/β ($)	0.02	0.13
	k_{eff}	1.000	1.001
	k_p	0.994	0.994
	M_T	155.3	174.6

It can be seen in Tables 9 and 10 that all of the detector systems compare very well with the desired configurations (all within 1 cent). It should also be noted that the reactor period calculated from the NPODs is always slightly higher than from the control rod worth curves or facility detectors (resulting in a slightly smaller reactor period).

Table 10. Results from the Godiva positive period configurations.

	Configuration	PP1	PP2	PP3
Desired configuration	Reactor Period (sec)	500	180	120
	ρ/β ($)	0.02	0.06	0.08
	k_{eff}	1.000	1.000	1.001
	k_p	0.994	0.994	0.994
	M_T	155.4	161.2	165.3
Startups (pulse mode)	Reactor Period (sec)	489	189	117
	ρ/β ($)	0.02	0.06	0.08
	k_{eff}	1.000	1.000	1.001
	k_p	0.994	0.994	0.994
	M_T	155.5	160.8	165.6
Linears (current mode)	Reactor Period (sec)	490	195	118
	ρ/β ($)	0.02	0.06	0.08
	k_{eff}	1.000	1.000	1.001
	k_p	0.994	0.994	0.994
	M_T	155.4	160.5	165.5
NPOD count rate	Reactor Period (sec)	546	208	133
	ρ/β ($)	0.02	0.05	0.08
	k_{eff}	1.000	1.000	1.000
	k_p	0.994	0.994	0.994
	M_T	155.1	160.0	164.1

5. CONCLUSIONS

Configurations on the CALIBAN and Godiva assemblies were measured using He-3 detector systems. These two fast burst assemblies are very similar and were compared. Measured configurations included many subcritical configurations at various reactivity states as well as configurations at and above delayed critical. The subcritical and delayed critical measurements were analyzed using the Feynman Variance-to-Mean method. It was found that the correlated neutron measurements compared quite well to the control rod worth curves and MCNP simulations. The largest Δk_{eff} between the measured data and the control rod worth curves was 0.008. The largest Δk_{eff} between the measured and simulated data was 0.009. Count rate measurements from the positive period configurations were also very accurate but correlated neutron analysis for these configurations was not successful.

In addition to the Godiva measurements in 2013, measurements were also performed on the Planet and Flat-Top critical assemblies at NCERC. Future work includes analysis and simulations of these measurements. Additional future work includes applying recent work on uncertainty analysis to the Caliban and Godiva measurements in order to determine the uncertainty in the singles counting rate, doubles counting rate, and leakage multiplication [19].

ACKNOWLEDGMENTS

We would like to thank the Valduc CALIBAN operations team. We would also like to thank LANL and NSTec personnel who supported the measurements at NCERC, particularly J. Koster, D. Hayes, D. Lewis, D. Rhodes, T. Beller, and P. Henning.

REFERENCES

[1] N. Authier and B. Mechitoua, ”Bare, Highly Enriched Uranium, Fast Burst Reactor CALIBAN”, ICSBEP Handbook, HMF-080 (2007).
[2] N. Authier, et. al., “Coupled Neutronic and Thermo-Mechanical Model of Super Prompt Pulsed Experiments at the Fast Burst Reactor CALIBAN,” ANIMMA, Marseille, France, June 7-10, 2009.
[3] J. Goda, “Godiva IV Critical Assembly Machine Reassembly and Startup,” ANS Winter Meeting, Washington DC, November 11-15, 2013.
[4] R. Mosteller, J. Goda, ”Godiva-IV Delayed-Critical Experiments and an Associated Prompt-Burst Experiment,” International Handbook of Evaluated Criticality Safety Benchmark Experiments, NEA/NSC/DOC/(95)03/I, HEU-MET-FAST-086.
[5] Personal communication with N. Authier, June 2012.
[6] G. R. Keepin, “Physics of Nuclear Kinetics,” 1965.
[7] A. Chapelle, et. al., “Joint Neutron Noise Measurements on Metallic Reactor Caliban,” ANIMMA, Marseille, France, June 23-27, 2013.
[8] D. Cifarelli, W. Hage, “Models for a Three-Parameter Analysis of Neutron Signal Correlation Measurements for Fissile Material Assay,” Nuc. Instr. Meth. A251, 550-563, 1986.
[9] M. Smith-Nelson, et. al., “Neutron Specialist Handbook and Informational Text,” LA-UR-07-6170, 2007.
[10] J. Mattingly, “Polyethylene-Reflected Plutonium Metal Sphere: Subcritical Neutron and Gamma Measurements,” SAND2009-5804, 2009.
[11] K. Butterfield, et. al., “Neutron Detection System Description,” LANL Report, 2006.
[12] A. Chapelle, P. Casoli, “Neutron Noise Measurements on Caliban Reactor: Kinetic Parameters and Associated Uncertainties Evaluation,” LANL/CEA Workshop, Los Alamos, NM, Nov. 29, 2012.
[13] A. Chapelle, et. al., “Joint Neutron Noise Measurements on Metallic Reactor Caliban,” Nuclear Data, New York, March 4-8, 2013.
[14] A. Chapelle, PHD Thesis, Caen University, 2014.
[15] J. Hutchinson, et. al., “Experimental Results of Joint LANL/CEA Measurements on CALIBAN,” ANS Annual Meeting, Atlanta, GA, June 17-21, 2013.
[16] J. Hutchinson, et. al., “CALIBAN Measurements Near Delayed Critical Using Subcritical Measurement Methods,” ANS Winter Meeting, Washington DC, November 11-15, 2013.
[17] J. Hutchinson, et. al., “LANL CALIBAN Subcritical Measurements,” LANL/CEA Workshop, Los Alamos, NM, November 29, 2012.
[18] Personal communication with A. Sood and N. Authier, June 2012.
[19] J. Hutchinson, et. al., “Uncertainty analysis of subcritical benchmark experiments using the Hage-Cifarelli formalism,” LA-UR-13-26060 (2013).

CALIBAN and Godiva IV Measurements Using Helium-3 Detector Systems

J. Hutchinson, A. Sood, M. Smith-Nelson, J. Goda, J. Bounds, W. Myers, T. Cutler, B. Richard, B. Rooney
Los Alamos National Laboratory

A. Chapelle, P. Casoli, N. Authier
Commissariat `a l'Energie Atomique et aux Energies Alternatives (CEA) Valduc

LA-UR-14-27372
Approved for public release;
distribution is unlimited.

Los Alamos NATIONAL LABORATORY EST. 1943
The World's Greatest Science Protecting America
NNSA

Background

- Two joint LANL/CEA measurement campaigns were performed:
  - Valduc, June 2012: Caliban
  - NCERC, July 2013: Godiva-IV, Planet (class foils), and Flat-Top (HEU core)
- Measured over 50 configurations between the 4 assemblies.
- This presentation will focus on comparing the Caliban and Godiva-IV measurements.

Background

- Several goals for measurements:
  - CEA research of neutron noise measurements (thesis work of Amaury Chapelle).
  - Validation of US work on subcritical experiments:
    - New simulation methods (MCNP list-mode patch)
    - New detector hardware
    - New analysis software
  - Provide additional measurements to compare Caliban and Godiva (the focus of this talk).

Detectors

- Four “main” detector systems used: 2 LANL NPOD detectors, one LANL SNAP detector, and one CEA detector system with three He-3 tubes inside polyethylene.
- All detectors were run remotely (from the control rooms).

CEA detector system

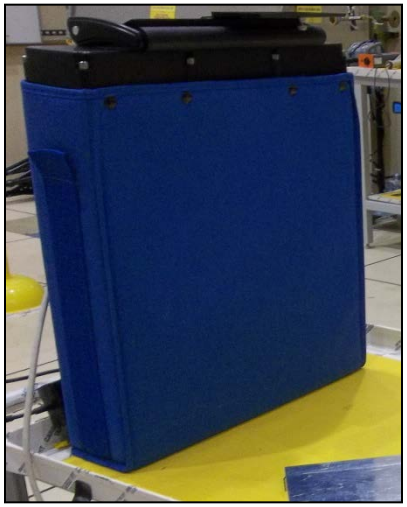

NPOD detector system

Caliban Overview

- Metallic cylindrical core
  - ^{235}U and Mo alloy
  - Diameter = 19.5 cm
  - Height = 25 cm
  - 113 kg of HEU
- 2 blocks
  - A mobile one (below)
  - A fixed one (above)
- 4 control rods
  - Same composition as the blocks
- Cylindrical central irradiation channel
- Described in HEU-MET-FAST-080

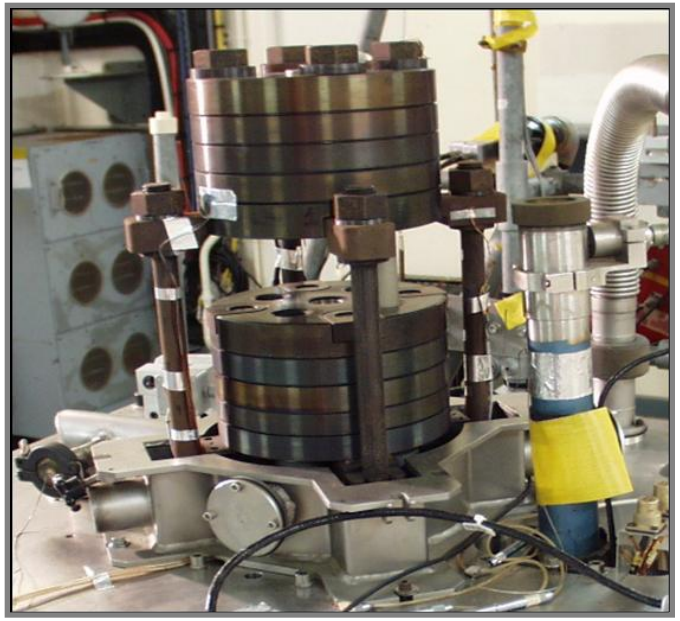

Godiva-IV Overview

- Cylindrical uranium metal fast burst assembly
- 65 kg, 93% enriched
- 7-inch diameter (17.8 cm), 6-inch tall (15.2 cm)
- Operates at delayed critical or prompt critical
- Maximum burst is approximately 90,000 MW_{th} with a full width half max (FWHM) pulse of 25 μs
- A burst was not performed for this measurement campaign
- Described in HEU-MET-FAST-086.

Comparison

- Comparison of the two assemblies

	Godiva IV	Caliban
U-235 wt.% percent	93.16	93.417
Mo wt.%	1.5	9.86
U mass (kg)	64.4	113
ID (cm)	*	3
OD (cm)	17.78	19.5
Height (cm)	15.59	25.2
Total number of rods	3	4
Control rod reactivity worth ($)	1.20	2.26
Assumed delayed neutron fraction	659 pcm	

*: Godiva-IV does not have a constant ID but on average it is less than the ID of Caliban

Caliban Configurations

		Element Positions (in mm)			
Configuration		SB position	BC1	BC2	BC3
SB out	S1	0.089	0.000	0.000	0.000
SB 10mm	S2	9.970	0.000	0.000	0.000
SB 20mm	S3	20.019	0.000	0.000	0.000
SB 40mm	S4	40.019	0.000	0.000	0.000
SB 60mm	S5	60.009	0.000	0.000	0.000
SB 65mm	S6	65.032	0.000	0.000	0.000
SB 67.5mm	S7	67.501	0.000	0.000	0.000
SB in	S8	70.531	0.000	0.000	0.000
300 cent subcritical	S9	70.529	5.550	90.850	6.080
200 cent subcritical	S10	70.530	120.000	82.630	5.710
150 cent subcritical	S11	70.531	120.000	118.510	6.100
100 cent subcritical	S12	70.531	205.120	69.900	7.000
80 cent subcritical	S13	70.531	205.100	87.700	6.790
delayed critical	DC1	70.532	205.120	69.970	110.000
delayed critical	DC2	70.531	205.100	87.700	96.200
500 second period	PP1	70.532	205.100	50.000	127.590
60 second period	PP2	70.532	205.100	50.000	135.590

Cf-252 source (1.14e6 n/s) placed in center of Caliban for all subcritical configurations.

Since Caliban is HEU there are few neutron emissions below delayed critical so a source is desired to increase counting statistics.

- 0 means element is fully withdrawn

Godiva-IV Configurations

		Element Positions (in inches)		
Configuration		SB position	CR1	CR2
SB out	S1	7.844	4.050	4.050
SB 2.083"	S2	2.083	4.050	4.050
SB 0.994"	S3	0.994	4.050	4.050
SB 0.544"	S4	0.544	4.050	4.050
SB 0.272"	S5	0.272	4.050	4.050
SB 0.161"	S6	0.161	4.050	4.050
SB in	S7	-0.130	4.050	4.050
200 cents subcritical	S8	-0.130	3.606	3.504
150 cents subcritical	S9	-0.130	2.258	2.448
100 cents subcritical	S10	-0.130	1.706	1.655
75 cents subcritical	S11	-0.130	1.344	1.304
50 cents subcritical	S12	-0.130	1.048	1.000
Delayed critical	DC1	-0.130	0.312	0.311
Delayed critical	DC2	-0.130	0.363	0.364
Delayed critical	DC3	-0.130	0.158	0.151
500 sec period	PP1	-0.130	0.097	0.151
180 sec period	PP2	-0.130	0.097	0.057
120 sec period	PP3	-0.130	0.023	0.057

Cf-252 source (2.24e5 n/s) placed in center of Godiva for all subcritical configurations, DC1, and DC2.

Since Godiva is HEU there are few neutron emissions below delayed critical so a source is desired to increase counting statistics.

Caliban and Godiva configurations ranged from -$20 to +$0.14.

- 0 (or negative number) means element is fully inserted

Analysis method

- NPOD produces list-mode data.
- Analyzed using “Momentum”
  - Hage-Cifarelli formalism used
  - Sequential binning
  - 512 gates of 4 micro-sec each
  - All data shown are asymptotic results (not using a particular gate width)
  - Nu-bar data used included Cf-252 starters and U-235 induced fission
- Total multiplication determined from leakage multiplication using the Serber equation (LA-335, 1945).
  - Note that this equation and calculation of keff require many assumptions (equivalent fundamental mode source, point source)
  - This work does not assess the validity of these assumptions.

Results

- Multiplication results.

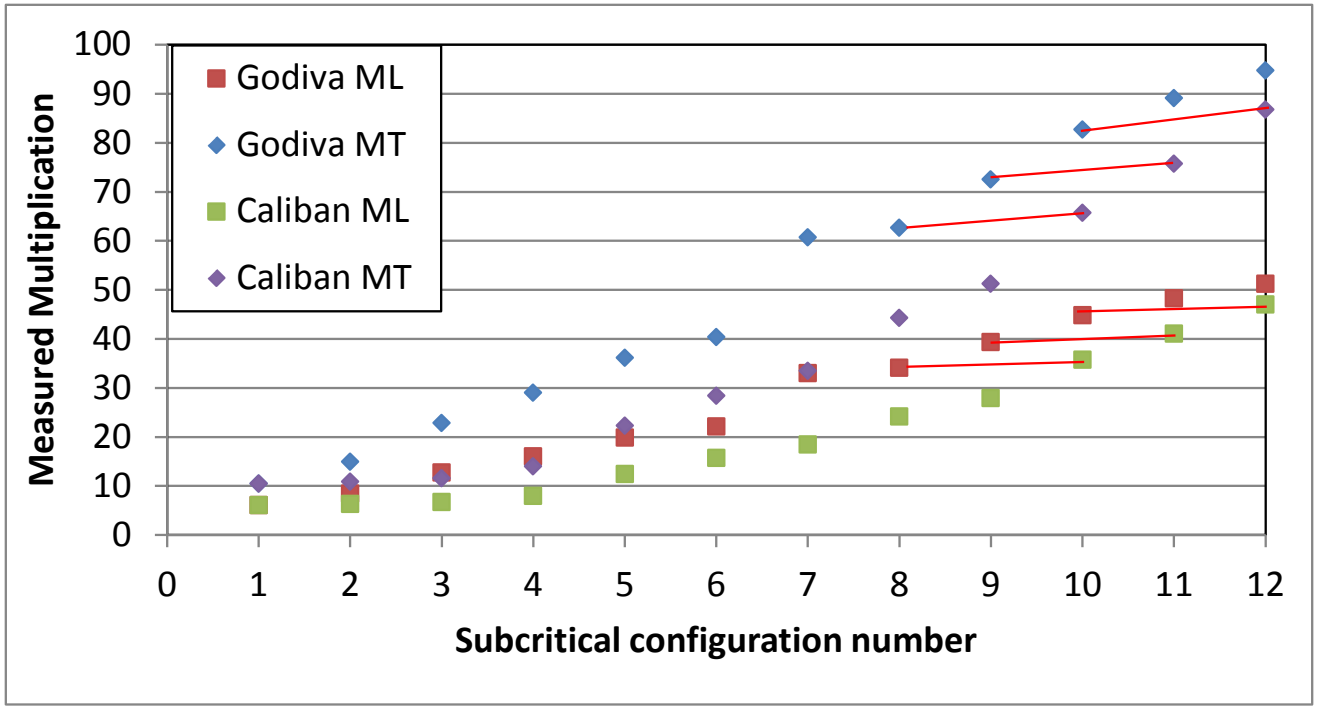

Results

- Results for configurations in which the control rods were out.

Assembly	SB Position	Configuration	M_T	keff	MCNP KCODE	C/E
Caliban	SB out	S1	10.5	0.910	0.881	0.968
	SB 10mm	S2	10.9	0.914		
	SB 20mm	S3	11.6	0.920	0.891	0.969
	SB 40mm	S4	13.9	0.934	0.909	0.973
	SB 60mm	S5	22.2	0.961	0.945	0.982
	SB 65mm	S6	28.3	0.971	0.958	0.986
	SB 67.5mm	S7	33.5	0.977	0.965	0.988
Godiva	SB out	S1	10.5	0.911	0.871	0.957
	SB 2.083"	S2	14.9	0.939	0.909	0.968
	SB 0.994"	S3	22.8	0.963	0.943	0.980
	SB 0.544"	S4	29.0	0.972	0.959	0.987
	SB 0.272"	S5	36.1	0.979	0.969	0.991
	SB 0.161"	S6	40.3	0.982	0.974	0.992

Comparisons to simulations get better as multiplication increases.

Godiva Results

	Configuration	S7	S8	S9	S10	S11	S12
Control rod worth curves	ρ/β ($)	-2.07	-2.00	-1.50	-1.00	-0.75	-0.50
	ρ	-0.014	-0.013	-0.010	-0.007	-0.005	-0.003
	k_{eff}	0.987	0.987	0.990	0.993	0.995	0.997
	k_p	0.980	0.980	0.984	0.987	0.989	0.990
	M_T	50.0	51.2	61.3	76.4	87.1	101.5
NPOD Feynman Analysis	M_T	60.7	62.6	72.5	82.7	89.1	94.7
	k_p	0.984	0.984	0.986	0.988	0.989	0.989
	k_{eff}	0.990	0.991	0.993	0.994	0.995	0.996
	C/E M_T	0.824	0.818	0.846	0.924	0.978	1.072
	C/E k	0.996	0.996	0.997	0.999	1.000	1.001
CEA detector	M_T	60.3	62.6	74.7	88.6	99.9	112.0
	k_p	0.983	0.984	0.987	0.989	0.990	0.991
	k_{eff}	0.990	0.991	0.993	0.995	0.997	0.998
	C/E M_T	0.830	0.819	0.821	0.862	0.873	0.907
	C/E k	0.997	0.996	0.997	0.998	0.999	0.999
MCNP KCODE (bias adjusted)	k_{eff}	0.986	0.987	0.990	0.993	0.995	0.996
	k_p	0.979	0.980	0.984	0.986	0.988	0.990
	M_T	48.0	50.3	60.7	73.2	85.5	97.0
	C/E M_T	1.042	1.019	1.010	1.043	1.019	1.046
	C/E k	1.001	1.000	1.000	1.001	1.000	1.000

From CR worth curves

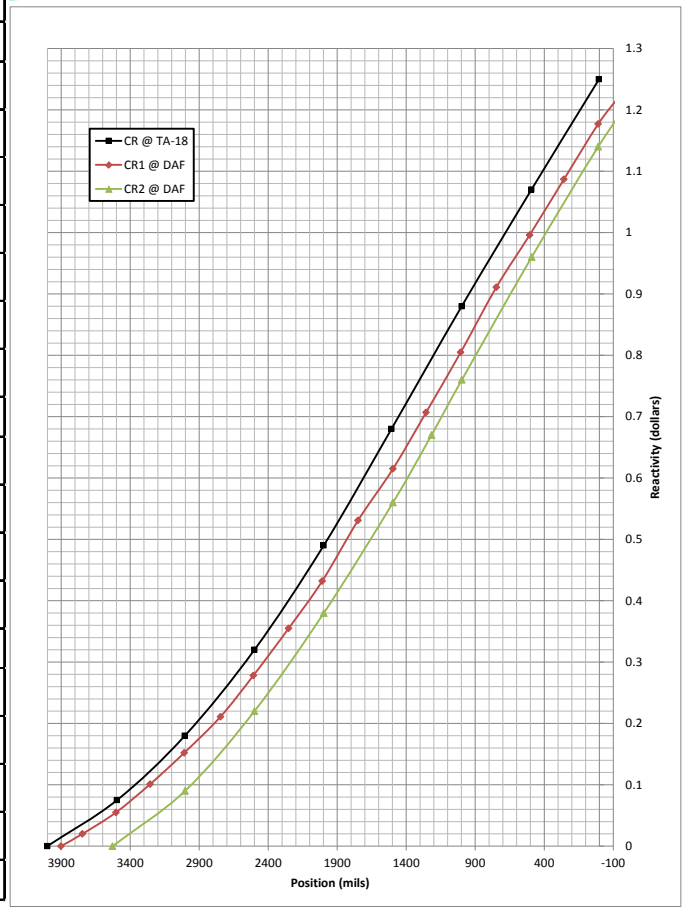

Los Alamos NATIONAL LABORATORY EST. 1943
The World's Greatest Science Protecting America
NNSA

Godiva Results

	Configuration	S7	S8	S9	S10	S11	S12
Control rod worth curves	ρ/β ($)	-2.07	-2.00	-1.50	-1.00	-0.75	-0.50
	ρ	-0.014	-0.013	-0.010	-0.007	-0.005	-0.003
	k_{eff}	0.987	0.987	0.990	0.993	0.995	0.997
	k_p	0.980	0.980	0.984	0.987	0.989	0.990
	M_T	50.0	51.2	61.3	76.4	87.1	101.5
NPOD Feynman Analysis	M_T	60.7	62.6	72.5	82.7	89.1	94.7
	k_p	0.984	0.984	0.986	0.988	0.989	0.989
	k_{eff}	0.990	0.991	0.993	0.994	0.995	0.996
	C/E M_T	0.824	0.818	0.846	0.924	0.978	1.072
	C/E k	0.996	0.996	0.997	0.999	1.000	1.001
CEA detector	M_T	60.3	62.6	74.7	88.6	99.9	112.0
	k_p	0.983	0.984	0.987	0.989	0.990	0.991
	k_{eff}	0.990	0.991	0.993	0.995	0.997	0.998
	C/E M_T	0.830	0.819	0.821	0.862	0.873	0.907
	C/E k	0.997	0.996	0.997	0.998	0.999	0.999
MCNP KCODE (bias adjusted)	k_{eff}	0.986	0.987	0.990	0.993	0.995	0.996
	k_p	0.979	0.980	0.984	0.986	0.988	0.990
	M_T	48.0	50.3	60.7	73.2	85.5	97.0
	C/E M_T	1.042	1.019	1.010	1.043	1.019	1.046
	C/E k	1.001	1.000	1.000	1.001	1.000	1.000

From CR worth curves

$\rho = (\rho/\beta_{eff}) \times \beta_{eff} = (\rho/\beta_{eff}) \times 0.00659$

Godiva Results

	Configuration	S7	S8	S9	S10	S11	S12
Control rod worth curves	ρ/β ($)	-2.07	-2.00	-1.50	-1.00	-0.75	-0.50
	ρ	-0.014	-0.013	-0.010	-0.007	-0.005	-0.003
	k_{eff}	0.987	0.987	0.990	0.993	0.995	0.997
	k_p	0.980	0.980	0.984	0.987	0.989	0.990
	M_T	50.0	51.2	61.3	76.4	87.1	101.5
NPOD Feynman Analysis	M_T	60.7	62.6	72.5	82.7	89.1	94.7
	k_p	0.984	0.984	0.986	0.988	0.989	0.989
	k_{eff}	0.990	0.991	0.993	0.994	0.995	0.996
	C/E M_T	0.824	0.818	0.846	0.924	0.978	1.072
	C/E k	0.996	0.996	0.997	0.999	1.000	1.001
CEA detector	M_T	60.3	62.6	74.7	88.6	99.9	112.0
	k_p	0.983	0.984	0.987	0.989	0.990	0.991
	k_{eff}	0.990	0.991	0.993	0.995	0.997	0.998
	C/E M_T	0.830	0.819	0.821	0.862	0.873	0.907
	C/E k	0.997	0.996	0.997	0.998	0.999	0.999
MCNP KCODE (bias adjusted)	k_{eff}	0.986	0.987	0.990	0.993	0.995	0.996
	k_p	0.979	0.980	0.984	0.986	0.988	0.990
	M_T	48.0	50.3	60.7	73.2	85.5	97.0
	C/E M_T	1.042	1.019	1.010	1.043	1.019	1.046
	C/E k	1.001	1.000	1.000	1.001	1.000	1.000

From CR worth curves

$\rho = (\rho/\beta_{eff}) \times \beta_{eff} = (\rho/\beta_{eff}) \times 0.00659$

$k_{eff} = 1/(1-\rho)$

Godiva Results

	Configuration	S7	S8	S9	S10	S11	S12
Control rod worth curves	ρ/β ($)	-2.07	-2.00	-1.50	-1.00	-0.75	-0.50
	ρ	-0.014	-0.013	-0.010	-0.007	-0.005	-0.003
	k_{eff}	0.987	0.987	0.990	0.993	0.995	0.997
	k_p	0.980	0.980	0.984	0.987	0.989	0.990
	M_T	50.0	51.2	61.3	76.4	87.1	101.5
NPOD Feynman Analysis	M_T	60.7	62.6	72.5	82.7	89.1	94.7
	k_p	0.984	0.984	0.986	0.988	0.989	0.989
	k_{eff}	0.990	0.991	0.993	0.994	0.995	0.996
	C/E M_T	0.824	0.818	0.846	0.924	0.978	1.072
	C/E k	0.996	0.996	0.997	0.999	1.000	1.001
CEA detector	M_T	60.3	62.6	74.7	88.6	99.9	112.0
	k_p	0.983	0.984	0.987	0.989	0.990	0.991
	k_{eff}	0.990	0.991	0.993	0.995	0.997	0.998
	C/E M_T	0.830	0.819	0.821	0.862	0.873	0.907
	C/E k	0.997	0.996	0.997	0.998	0.999	0.999
MCNP KCODE (bias adjusted)	k_{eff}	0.986	0.987	0.990	0.993	0.995	0.996
	k_p	0.979	0.980	0.984	0.986	0.988	0.990
	M_T	48.0	50.3	60.7	73.2	85.5	97.0
	C/E M_T	1.042	1.019	1.010	1.043	1.019	1.046
	C/E k	1.001	1.000	1.000	1.001	1.000	1.000

From CR worth curves

$\rho = (\rho/\beta_{eff}) \times \beta_{eff} = (\rho/\beta_{eff}) \times 0.00659$

$k_{eff} = 1/(1-\rho)$

$k_p = k_{eff}(1-\beta_{eff}) = k_{eff}(1-0.00659)$

Godiva Results

	Configuration	S7	S8	S9	S10	S11	S12
Control rod worth curves	ρ/β ($)	-2.07	-2.00	-1.50	-1.00	-0.75	-0.50
	ρ	-0.014	-0.013	-0.010	-0.007	-0.005	-0.003
	k_{eff}	0.987	0.987	0.990	0.993	0.995	0.997
	k_p	0.980	0.980	0.984	0.987	0.989	0.990
	M_T	50.0	51.2	61.3	76.4	87.1	101.5
NPOD Feynman Analysis	M_T	60.7	62.6	72.5	82.7	89.1	94.7
	k_p	0.984	0.984	0.986	0.988	0.989	0.989
	k_{eff}	0.990	0.991	0.993	0.994	0.995	0.996
	C/E M_T	0.824	0.818	0.846	0.924	0.978	1.072
	C/E k	0.996	0.996	0.997	0.999	1.000	1.001
CEA detector	M_T	60.3	62.6	74.7	88.6	99.9	112.0
	k_p	0.983	0.984	0.987	0.989	0.990	0.991
	k_{eff}	0.990	0.991	0.993	0.995	0.997	0.998
	C/E M_T	0.830	0.819	0.821	0.862	0.873	0.907
	C/E k	0.997	0.996	0.997	0.998	0.999	0.999
MCNP KCODE (bias adjusted)	k_{eff}	0.986	0.987	0.990	0.993	0.995	0.996
	k_p	0.979	0.980	0.984	0.986	0.988	0.990
	M_T	48.0	50.3	60.7	73.2	85.5	97.0
	C/E M_T	1.042	1.019	1.010	1.043	1.019	1.046
	C/E k	1.001	1.000	1.000	1.001	1.000	1.000

From CR worth curves

$\rho = (\rho/\beta_{eff}) \times \beta_{eff} = (\rho/\beta_{eff}) \times 0.00659$

$k_{eff} = 1/(1-\rho)$

$k_p = k_{eff}(1-\beta_{eff}) = k_{eff}(1-0.00659)$

$M_T = 1/(1-k_p)$

Godiva Results

	Configuration	S7	S8	S9	S10	S11	S12
Control rod worth curves	ρ/β ($)	-2.07	-2.00	-1.50	-1.00	-0.75	-0.50
	ρ	-0.014	-0.013	-0.010	-0.007	-0.005	-0.003
	k_{eff}	0.987	0.987	0.990	0.993	0.995	0.997
	k_p	0.980	0.980	0.984	0.987	0.989	0.990
	M_T	50.0	51.2	61.3	76.4	87.1	101.5
NPOD Feynman Analysis	M_T	60.7	62.6	72.5	82.7	89.1	94.7
	k_p	0.984	0.984	0.986	0.988	0.989	0.989
	k_{eff}	0.990	0.991	0.993	0.994	0.995	0.996
	C/E M_T	0.824	0.818	0.846	0.924	0.978	1.072
	C/E k	0.996	0.996	0.997	0.999	1.000	1.001
CEA detector	M_T	60.3	62.6	74.7	88.6	99.9	112.0
	k_p	0.983	0.984	0.987	0.989	0.990	0.991
	k_{eff}	0.990	0.991	0.993	0.995	0.997	0.998
	C/E M_T	0.830	0.819	0.821	0.862	0.873	0.907
	C/E k	0.997	0.996	0.997	0.998	0.999	0.999
MCNP KCODE (bias adjusted)	k_{eff}	0.986	0.987	0.990	0.993	0.995	0.996
	k_p	0.979	0.980	0.984	0.986	0.988	0.990
	M_T	48.0	50.3	60.7	73.2	85.5	97.0
	C/E M_T	1.042	1.019	1.010	1.043	1.019	1.046
	C/E k	1.001	1.000	1.000	1.001	1.000	1.000

From CR worth curves

$\rho = (\rho/\beta_{eff}) \times \beta_{eff} = (\rho/\beta_{eff}) \times 0.00659$

$k_{eff} = 1/(1-\rho)$

$k_p = k_{eff}(1-\beta_{eff}) = k_{eff}(1-0.00659)$

$M_T=1/(1-k_p)$

Calculated from measured data

Godiva Results

	Configuration	S7	S8	S9	S10	S11	S12
Control rod worth curves	ρ/β ($)	-2.07	-2.00	-1.50	-1.00	-0.75	-0.50
	ρ	-0.014	-0.013	-0.010	-0.007	-0.005	-0.003
	k_{eff}	0.987	0.987	0.990	0.993	0.995	0.997
	k_p	0.980	0.980	0.984	0.987	0.989	0.990
	M_T	50.0	51.2	61.3	76.4	87.1	101.5
NPOD Feynman Analysis	M_T	60.7	62.6	72.5	82.7	89.1	94.7
	k_p	0.984	0.984	0.986	0.988	0.989	0.989
	k_{eff}	0.990	0.991	0.993	0.994	0.995	0.996
	C/E M_T	0.824	0.818	0.846	0.924	0.978	1.072
	C/E k	0.996	0.996	0.997	0.999	1.000	1.001
CEA detector	M_T	60.3	62.6	74.7	88.6	99.9	112.0
	k_p	0.983	0.984	0.987	0.989	0.990	0.991
	k_{eff}	0.990	0.991	0.993	0.995	0.997	0.998
	C/E M_T	0.830	0.819	0.821	0.862	0.873	0.907
	C/E k	0.997	0.996	0.997	0.998	0.999	0.999
MCNP KCODE (bias adjusted)	k_{eff}	0.986	0.987	0.990	0.993	0.995	0.996
	k_p	0.979	0.980	0.984	0.986	0.988	0.990
	M_T	48.0	50.3	60.7	73.2	85.5	97.0
	C/E M_T	1.042	1.019	1.010	1.043	1.019	1.046
	C/E k	1.001	1.000	1.000	1.001	1.000	1.000

From CR worth curves

$\rho = (\rho/\beta_{eff}) \times \beta_{eff} = (\rho/\beta_{eff}) \times 0.00659$

$k_{eff} = 1/(1-\rho)$

$k_p = k_{eff}(1-\beta_{eff}) = k_{eff}(1-0.00659)$

$M_T=1/(1-k_p)$

Calculated from measured data

Godiva Results

	Configuration	S7	S8	S9	S10	S11	S12
Control rod worth curves	ρ/β ($)	-2.07	-2.00	-1.50	-1.00	-0.75	-0.50
	ρ	-0.014	-0.013	-0.010	-0.007	-0.005	-0.003
	k_{eff}	0.987	0.987	0.990	0.993	0.995	0.997
	k_p	0.980	0.980	0.984	0.987	0.989	0.990
	M_T	50.0	51.2	61.3	76.4	87.1	101.5
NPOD Feynman Analysis	M_T	60.7	62.6	72.5	82.7	89.1	94.7
	k_p	0.984	0.984	0.986	0.988	0.989	0.989
	k_{eff}	0.990	0.991	0.993	0.994	0.995	0.996
	C/E M_T	0.824	0.818	0.846	0.924	0.978	1.072
	C/E k	0.996	0.996	0.997	0.999	1.000	1.001
CEA detector	M_T	60.3	62.6	74.7	88.6	99.9	112.0
	k_p	0.983	0.984	0.987	0.989	0.990	0.991
	k_{eff}	0.990	0.991	0.993	0.995	0.997	0.998
	C/E M_T	0.830	0.819	0.821	0.862	0.873	0.907
	C/E k	0.997	0.996	0.997	0.998	0.999	0.999
MCNP KCODE (bias adjusted)	k_{eff}	0.986	0.987	0.990	0.993	0.995	0.996
	k_p	0.979	0.980	0.984	0.986	0.988	0.990
	M_T	48.0	50.3	60.7	73.2	85.5	97.0
	C/E M_T	1.042	1.019	1.010	1.043	1.019	1.046
	C/E k	1.001	1.000	1.000	1.001	1.000	1.000

Measurements are generally over-predicting M and k versus CR calibration.

Greatest Δk_{eff} = 0.004 between NPOD measurements and CR curves (0.991 – 0.987).

In general the agreement is slightly better as the reactivity increases.

Bias was determined from ICSBEP benchmark configuration at DC.

Assumed to be constant for all configurations.

Caliban Results

	Configuration	S8	S9	S10	S11	S12
Control rod worth curves	ρ/β ($)	-3.72	-3.00	-2.00	-1.50	-1.00
	ρ	-0.025	-0.020	-0.013	-0.010	-0.007
	k_{eff}	0.976	0.981	0.987	0.990	0.993
	k_p	0.970	0.974	0.980	0.984	0.987
	M_T	32.9	38.7	51.2	61.3	76.4
NPOD Feynman Analysis	M_T	44.2	51.2	65.7	75.7	86.7
	k_p	0.977	0.980	0.985	0.987	0.988
	k_{eff}	0.984	0.987	0.991	0.993	0.995
	C/E M_T	0.745	0.756	0.780	0.809	0.881
	C/E k	0.992	0.994	0.996	0.997	0.998
MCNP KCODE (bias adjusted)	k_{eff}	0.975	0.981	0.988	0.991	0.993
	k_p	0.969	0.974	0.981	0.984	0.986
	M_T	31.8	39.1	53.0	63.0	73.5
	C/E M_T	1.037	0.991	0.967	0.973	1.039
	C/E k	1.001	1.000	0.999	1.000	1.001

Greatest Δk_{eff} = 0.008 between NPOD measurements and CR curves (0.984 – 0.970).

Results

- Comparison of Godiva IV and Caliban results.

	Assembly	Godiva	CALIBAN	Godiva	CALIBAN	Godiva	CALIBAN
Control rod worth curves	ρ/β ($)	-2.00		-1.50		-1.00	
	ρ	-0.013		-0.010		-0.007	
	k_{eff}	0.987		0.990		0.993	
	k_p	0.980		0.984		0.987	
	M_T	51.2		61.3		76.4	
NPOD Feynman Analysis	M_T	62.6	65.7	72.5	75.7	82.7	86.7
	k_p	0.984	0.985	0.986	0.987	0.988	0.988
	k_{eff}	0.991	0.991	0.993	0.993	0.994	0.995
	C/E M_T	0.818	0.780	0.846	0.809	0.924	0.881
	C/E k	0.996	0.996	0.997	0.997	0.999	0.998

Results from Godiva and Caliban were very similar.

Both tended to over predict M (and subsequently k) compared with the CR worth curves.

Since Godiva gave slightly lower multiplication values it compares to the CR worth curves a little better than the Caliban results.

Results: Delayed Critical

	Assembly	CALIBAN	Godiva	CALIBAN	Godiva
	Configuration	DC1	DC2	DC2	DC3
	Position	2	-	1	-
	Cf source	Yes	Yes	No	No
Delayed critical definition	ρ/β ($)	0			
	ρ	0			
	k_{eff}	1.000			
	k_p	0.993			
	M_T	151.7			
NPOD Feynman Analysis	M_T	170.9	182.4	177.1	127.7
	k_p	0.994	0.995	0.994	0.992
	k_{eff}	1.001	1.001	1.001	0.999
	ρ	7.43E-04	1.11E-03	9.49E-04	-1.25E-03
	ρ/β ($)	0.11	0.17	0.14	-0.19
	C/E M_T	0.888	0.832	0.857	1.189
	C/E k	0.999	0.999	0.999	1.001
MCNP KCODE (bias adjusted)	k_{eff}	0.999	1.000	1.000	1.001
	k_p	0.992	0.993	0.993	0.994
	M_T	131.7	144.3	152.2	165.5
	C/E M_T	1.152	1.051	0.997	0.917
	C/E k	1.001	1.000	1.000	0.999

All measured data compared well (within 150 pcm of the delayed critical definition).

Measured and simulated results were within 200 pcm.

Results: Delayed Critical

Count rate of facility detectors for Godiva DC configurations.

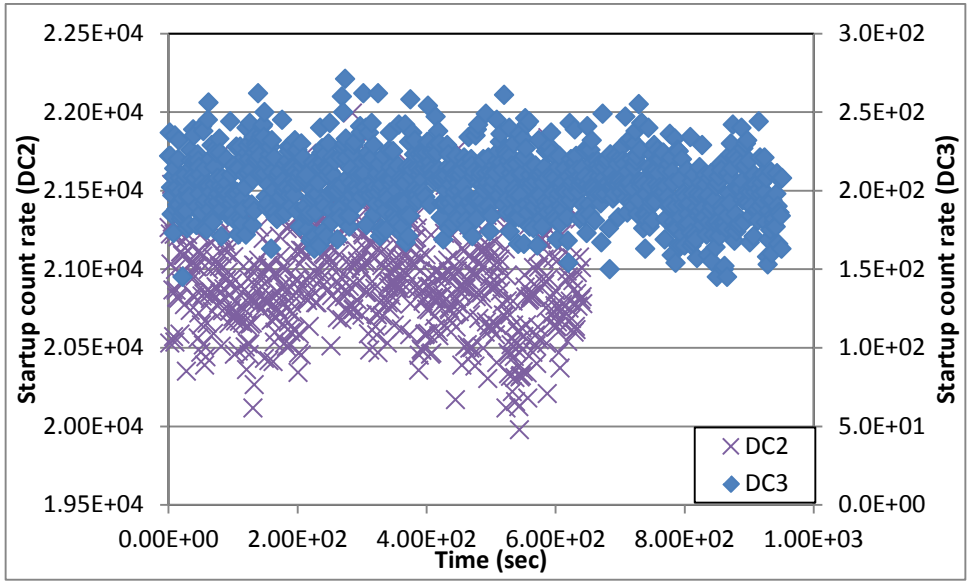

Using count rate data: both the NPOD and facility detectors showed that all four configurations were within 1 cent of delayed critical.

When the system is at delayed critical, $k_p = k_{eff}(1-\beta_{eff}) = 1-\beta_{eff}$.

Therefore one can used the measured k_p value to determine $\beta_{eff.}$

Source	Caliban	Godiva	Assumed
Yes	585	548	659
No	565	783	

Caliban Results: Positive Period

	Configuration	PP1	PP2
Desired configuration	Reactor Period (sec)	500	60
	ρ/β ($)	0.02	0.14
	k_{eff}	1.000	1.001
	k_p	0.994	0.994
	M_T	155.5	177.1
Valduc detectors	Reactor Period (sec)	508	61
	ρ/β ($)	0.02	0.14
	k_{eff}	1.000	1.001
	k_p	0.994	0.994
	M_T	155.4	176.8
NPOD count rate	Reactor Period (sec)	526	68
	ρ/β ($)	0.02	0.13
	k_{eff}	1.000	1.001
	k_p	0.994	0.994
	M_T	155.3	174.6

All of the detector systems compare very well with the desired configurations (all within 1 cent).

The reactor period calculated from the NPODs is always slightly higher than from the control rod worth curves or facility detectors (resulting in a slightly smaller reactivity).

Correlated neutron analysis was unsuccessful above delayed critical. A fit of count rates was used instead.

Godiva Results: Positive Period

	Configuration	PP1	PP2	PP3
Desired configuration	Reactor Period (sec)	500	180	120
	ρ/β ($)	0.02	0.06	0.08
	k_{eff}	1.000	1.000	1.001
	k_p	0.994	0.994	0.994
	M_T	155.4	161.2	165.3
Startups (pulse mode)	Reactor Period (sec)	489	189	117
	ρ/β ($)	0.02	0.06	0.08
	k_{eff}	1.000	1.000	1.001
	k_p	0.994	0.994	0.994
	M_T	155.5	160.8	165.6
Linears (current mode)	Reactor Period (sec)	490	195	118
	ρ/β ($)	0.02	0.06	0.08
	k_{eff}	1.000	1.000	1.001
	k_p	0.994	0.994	0.994
	M_T	155.4	160.5	165.5
NPOD count rate	Reactor Period (sec)	546	208	133
	ρ/β ($)	0.02	0.05	0.08
	k_{eff}	1.000	1.000	1.000
	k_p	0.994	0.994	0.994
	M_T	155.1	160.0	164.1

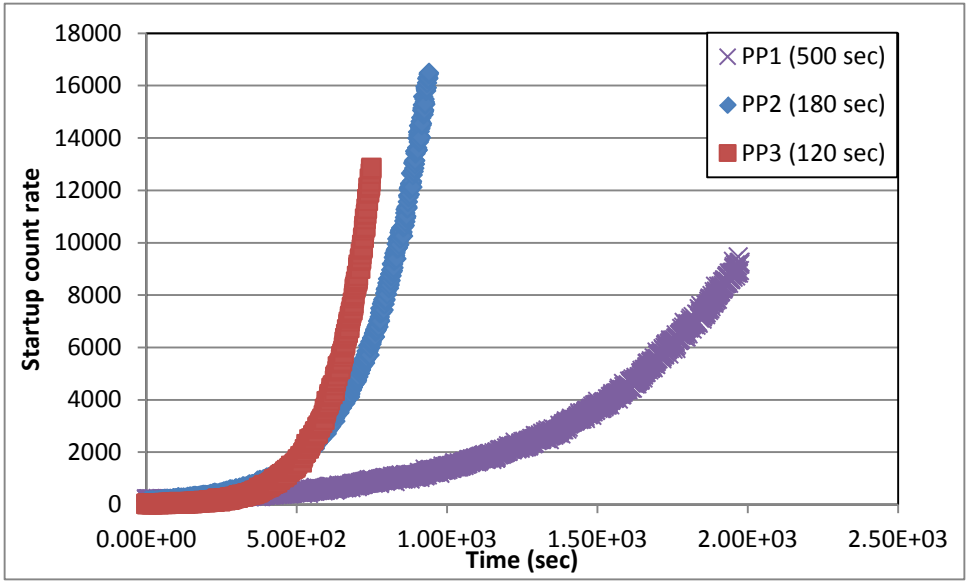

Conclusions and Future Work

- Conclusions
  - Joint CEA/LANL measurements performed on four critical assembly machines (this work only focused on Caliban and Godiva-IV results).
  - Results were very favorable for configurations in which the safety block was fully inserted for each assembly.
  - Results at and above delayed critical were also presented.
- Future Work
  - Document list-mode simulations for all configurations.
  - Analyze Planet and Flat-Top results (“best” nubar for Flat-Top?).
  - Investigate SCRAM and other measurements.

Documents related to this collaboration

- A. Chapelle, P. Casoli, “Neutron Noise Measurements on Caliban Reactor: Kinetic Parameters and Associated Uncertainties Evaluation,” LANL/CEA Workshop, Los Alamos, NM, Nov. 29, 2012.
- J. Hutchinson, et. al., “LANL CALIBAN Subcritical Measurements,” LANL/CEA Workshop, Los Alamos, NM, November 29, 2012.
- A. Chapelle, et. al., “Joint Neutron Noise Measurements on Metallic Reactor Caliban,” Nuclear Data, New York, March 4-8, 2013.
- J. Hutchinson, et. al., “Experimental Results of Joint LANL/CEA Measurements on CALIBAN,” ANS Annual Meeting, Atlanta, GA, June 17-21, 2013.
- A. Chapelle, et. al., “Joint Neutron Noise Measurements on Metallic Reactor Caliban,” ANIMMA, Marseille, France, June 23-27, 2013.
- J. Hutchinson, et. al., “CALIBAN Measurements Near Delayed Critical Using Subcritical Measurement Methods,” ANS Winter Meeting, Washington DC, November 11-15, 2013.
- B. Richard, et. al., “Simulation of Subcritical Neutron Noise Measurements on Caliban,” Draft.
- A. Chapelle, PHD Thesis, Caen University, May 12, 2014.
- J. Hutchinson, et. al., “Joint LANL/CEA Measurements on Godiva IV,” ANS Annual Meeting, Reno NV, June 16-19, 2014.

Documents related to this collaboration

- A. Chapelle, PHD Thesis, Caen University, May 12, 2014.
- Best source of information regarding recent CEA and LANL neutron noise measurements.

UNICAEN université de Caen Basse-Normandie

Normandie Université

Université de Caen Basse-Normandie

Ecole doctorale *SIMEM – Sciences des Structures, de l'Information, de la Matière Et des Matériaux*

Thèse de doctorat

présentée et soutenue le : *12/05/2014*

par

Amaury Chapelle

pour obtenir le

Doctorat de l'Université de Caen Basse-Normandie

Spécialité : *TH211, Constituants élémentaires et physique théorique*

Mesures de bruit neutronique auprès des réacteurs
Caliban, Godiva IV, Planet et Flattop
Détermination des paramètres cinétiques et des incertitudes associées

Directeur de thèse : *Professeur Gilles Ban*

Jury

Paul Reuss, professeur INSTN (rapporteur)
Pablo Rubiolo, professeur des universités, PHELMA Grenoble (rapporteur)
Hugues Delorme, enseignant de neutronique / maître de conférence, Ecole des Applications Militaires de l'Energie Atomique (EAMEA)
Pierre Casoli, Ingénieur chercheur, CEA, centre de Valduc
Nicolas Authier, Ingénieur chercheur, CEA, centre de Valduc
Gilles Ban, professeur des universités, ENSICAEN (directeur de thèse)

Jury invité :

Jesson Hutchinson, chercheur, Los Alamos National Laboratory
Capitaine de vaisseau Frédéric Janci, commandant l'Ecole des Applications Militaires de l'Energie Atomique (EAMEA)

Team for Valduc Measurement Campaign: June 2012

Los Alamos NATIONAL LABORATORY EST. 1943
The World's Greatest Science Protecting America
NNSA

Team for NCERC Measurement Campaign: July 2013

From left to right: Avneet Sood, David Hayes, Jesson Hutchinson, Mark Smith-Nelson, Joetta Goda, Pierre Casoli, John Bounds, Rene Sanchez, and Amaury Chapelle.

Acknowledgement

- This work was supported in part by the DOE Nuclear Criticality Safety Program, funded and managed by the National Nuclear Security Administration for the Department of Energy.

Hutchinson, Jesson D

From: Goda, Joetta Marie
Sent: Thursday, October 09, 2014 1:56 PM
To: Matzkin-Bridger, Ross
Cc: Klein, Steven Karl; Hayes, David Kirk; Sanchez, Rene Gerardo; Hutchinson, Jesson D
Subject: Tokai Visit

Ross,

Rene Sanchez, Jesson Hutchinson and I had a productive visit to the JAEA facility in Tokai last week. It was great to meet additional members of their team in person. Nishihara-san prepared meeting minutes which I assume he will send to you. If not, I can supply them. The facility tour was also very interesting and helpful. They seem to have a well-run facility.

Iwamoto-san presented a new variation on the Comet-Zeus configurations for the Lead void experiments. We made some suggestion based on the physical constraints of loading the fuel, but otherwise agree that it is a good approach. We agreed to narrow down to two configurations and both teams do calculations which can be compared in detail. They seemed surprised that we had ordered the lead already, but I explained our fiscal year end and that we can supplement the order if particular different size is indicated . As I'm sure you know, their fiscal year starts April 1 and they thought sometime in the following summer months would be good for them to send someone to Nevada to observe the experiments(lead void) and analyze data. We also learned that Iwamoto-san had spent 3 months at Los Alamos in the nuclear data group and knew some of our colleagues there.

Fukushima-san presented a series of experiments for reaction rates/sample worth that were done in the FCA. A clear experiment design for minor actinides has not yet emerged although we discussed many possibilities and exchanged information on fission chambers and samples. Our team will meet and brainstorm in light of the additional information showing where the largest calculation to experiment differences were.

Thank you for your support in sending Rene and Jesson to the conference and for your support of the facility visit. It is invaluable to meet and see things first-hand. Nishihara-san suggested a follow-up VCR, but Tsujimoto-san felt strongly that we should continue to communicate by email.

When do you anticipate the FY15 allocation arriving at the lab? I will budget the remaining FY14 funds accordingly as I get people started on the next phase. Let me know when you would like a schedule and I will incorporate what was discussed in Tokai.

~Joetta